agronomy

MDPI

Article

Profiling of the Salt Stress Responsive MicroRNA Landscape of C4 Genetic Model Species *Setaria viridis* (L.) Beauv

Joseph L. Pegler, Duc Quan Nguyen, Christopher P.L. Grof † and Andrew L. Eamens *,†

Centre For Plant Science, School of Environmental and Life Sciences, Faculty of Science, University of Newcastle, Callaghan, NSW 2308, Australia; Joseph.Pegler@uon.edu.au (J.L.P.); DucQuan.Nguyen@uon.edu.au (D.Q.N); Chris.Grof@newcastle.edu.au (C.P.L.G.)

* Correspondence: andy.eamens@newcastle.edu.au; Tel.: +61-249-217-784

† These authors have contributed equally to this work.

Received: 30 April 2020; Accepted: 8 June 2020; Published: 12 June 2020

Abstract: *Setaria viridis* has recently emerged as an ideal model species to genetically characterize the C_4 monocotyledonous grasses via a molecular modification approach. Soil salinization has become a compelling agricultural problem globally with salinity adversely impacting the yield potential of many of the major cereals. Small regulatory molecules of RNA, termed microRNAs (miRNAs), were originally demonstrated crucial for developmental gene expression regulation in plants, however, miRNAs have since been shown to additionally command a central regulatory role in abiotic stress adaptation. Therefore, a small RNA sequencing approach was employed to profile the salt stress responsive miRNA landscapes of the shoot and root tissues of two *Setaria viridis* accessions (A10 and ME034V) amenable to molecular modification. Small RNA sequencing-identified abundance alterations for miRNAs, miR169, miR395, miR396, miR397, miR398 and miR408, were experimentally validated via RT-qPCR. RT-qPCR was further applied to profile the molecular response of the miR160 and miR167 regulatory modules to salt stress. This analysis revealed accession- and tissue-specific responses for the miR160 and miR167 regulatory modules in A10 and ME034V shoot and root tissues exposed to salt stress. The findings reported here form the first crucial step in the identification of the miRNA regulatory modules to target for molecular manipulation to determine if such modification provides *S. viridis* with an improved tolerance to salt stress.

Keywords: *Setaria viridis*; salt stress; microRNA (miRNA) abundance; high throughput small RNA sequencing; RT-qPCR

1. Introduction

The global population continues to increase, and with this has come intensive urbanization and the greatly accelerated consumption of fossil fuels. In an attempt to supply food and fuel resources for the world's expanding population, the global land cover has been extensively modified over the last 50 years, with an alarming transition from the historical clearing of grasslands and savannas, to the current practice of clearing biodiverse landscapes in an attempt to address these continuing food and fuel supply demands [1–3]. Together, agriculture and industry, for food and fuel production, respectively, have significantly contributed to the global carbon footprint, which has, in turn, dramatically accelerated anthropogenic climate change [1,3,4]. Presently, the environmental issues associated with anthropogenically driven climate change, including altered precipitation patterns leading to drought and flood events, as well as soil salinity and nutrient imbalances and heat and cold stresses, have all increased in frequency, duration and severity of impact. Together, these changes have adversely affected the global crop yield [1,5,6]. Due to their sessile nature, plants have evolved

intricate and interrelated gene regulatory networks to mount adaptive responses to a diverse array of environmental constraints, adaptive responses largely initiated to limit the degree to which vegetative and/or reproductive development and productivity (i.e., yield) is compromised [3,7–12]. However, directly stemming from anthropogenically driven climate change, the increased severity of both the frequency and duration of climatic events that challenge the continued productivity of the agricultural industry has now far surpassed the rate at which key crop species can naturally evolve new genetic mechanisms to combat environmental stress.

Excluding natural climatic and topographic contributions, soil salinization is one abiotic stress greatly enhanced by the destructive impact of human activities, be they unfavorable farming practices, including illogical irrigation application, excessive fertilization and ploughing, or the pollution generated by industry [5,10,11,13]. Soil salinization has become a compelling agricultural problem globally with numerous studies demonstrating salinity to adversely impact the yield of the major cereal crops, wheat (*Triticum aestivum*), maize (*Zea mays*) and rice (*Oryza sativa*) [2,4,11–13]. Approximately 6% of the world's land (~800 million hectares) is now classed as being 'saline', including 80 million hectares of the arable land currently under irrigation (~20% of all irrigated farmland) [2,4,12]. Saline soils are unsuitable for the cultivation of most crop species due to the increased concentration of sodium (Na^+) and chloride (Cl^-) ions taken up by the roots, ions which are subsequently further concentrated in the aerial tissues [10,14]. An overabundance of Na^+ and/or Cl^- ions in plant leaf cells inhibits photosynthesis and the assimilation of carbon, both of which lead to the overall inhibition of plant growth [11,12,15,16]. In salt stressed tomato (*Solanum lycopersicum*) and common bean (*Phaseolus vulgaris*) for example, reduced photosynthetic potential is the result of defective chloroplast structures, and therefore, decreased chlorophyll content [12,17–19]. In addition to impacting photosynthesis and carbon assimilation, salt stress also negatively affects the key biological processes of protein synthesis and energy and lipid metabolism [11,12,16,20–23].

The global population is heavily reliant on the major monocotyledonous (monocot) grass cereals, rice, wheat and maize, all of which belong to the Poaceae family, for their daily calorific requirements [24,25]. Monocot grasses not only act as the primary sustenance source for humans, but other Poaceae family members such as rye (*Secale cereale*) and fescue (*Festuca arundinacea*) dominate agricultural pastures used to feed livestock [24,26]. Furthermore, the additional family members, sorghum (*Sorghum bicolor*), sugarcane (*Saccharum officinarum*), switchgrass (*Panicum virgatum*) and *Miscanthus* × *giganteus*, contribute the majority of plant material for biofuel production [27–31]. Due to their unique leaf anatomy, which enables efficient CO_2 fixation into biomass, even in less favorable growth environments of intense light and elevated temperature, C_4 plants such as maize, sorghum, sugarcane and switchgrass, are some of the most productive plant species [32]. Pearl millet (*Pennisetum glaucum*) and foxtail millet (*Setaria italica*) are particularly important members of the Poaceae family, and further, due to their utilization of the C_4 photosynthetic pathway, are widely cultivated in marginal lands frequently prone to abiotic stress [1,6–9,11,33]. In India, China and Japan, for example, *S. italica* is predominantly cultivated in dry regions with inadequate irrigation and saline soils [1,6,8,9,33,34], and due to its drought tolerance and rich provision of nutrient elements, *S. italica* represents an ancient grain crop that has been cultivated for over 7,000 years in China [6,7,35–37]. *Setaria viridis* (green foxtail) is a closely related wild ancestor of *S. italica*, and with both of these *Setaria* species forming a conserved phylogenetic relationship to numerous agronomically important C_4 species, *S. viridis* has recently emerged as a potential model for the genetic characterization of the photosynthesis and cell wall biology pathways that are unique to the C_4 monocot grasses [27–29,38–41]. More recently, *S. viridis* has been demonstrated to be readily amenable to molecular manipulation via *Agrobacterium tumefaciens* (*Agrobacterium*)-mediated transformation [42–45], a demonstration that adds considerable weight to its use as a genetic model species to characterize C_4 monocot grass biology.

Plant microRNAs (miRNAs) are a class of small regulatory RNA, predominantly 21 nucleotides (nt) in length, processed from non-protein-coding RNA precursor transcripts transcribed from *MICRORNA* (*MIR*) loci by RNA polymerase II (Pol II) [46,47]. Post Pol II transcription, the miRNA precursor

transcript folds back on to itself to form a stem-loop structure of imperfectly double-stranded RNA (dsRNA) [48–50]. Following dsRNA formation, miRNA precursor transcripts are processed by the machinery proteins of the plant miRNA pathway, including SERRATE (SE), dsRNA BINDING1 (DRB1), DICER-LIKE1 (DCL1) and ARGONAUTE1 (AGO1) (reviewed in [51]). Post production, the mature miRNA is loaded by AGO1 to form the catalytic core of the miRNA-directed RNA-induced silencing complex (miRISC) [52], with miRISC using the loaded miRNA as a sequence specificity guide to target protein-coding messenger RNA (mRNA) transcripts to regulate (repress) target gene expression [52–54]. Initially, plant miRNAs were established as key regulators of gene expression throughout all phases of vegetative and reproductive development [47,53,55,56]; more recently however, plant miRNAs have been assigned roles in mediating a defense response against invading pathogens [57,58], or to direct the adaptive response of a plant to abiotic stress [59–62]. At the DNA sequence level, the structure of a *MIR* gene mirrors that of a protein coding gene consisting of a promoter region, coding sequence, and a terminator sequence [5,63,64]. Like those of protein coding genes, *MIR* gene promoter regions harbor numerous *cis*-regulatory elements (*CRE*s) with some of these responsive to environmental signals external to the cell and which contribute to the control of *MIR* gene expression, and hence, mature miRNA small RNA (sRNA) abundance [5,63,64]. Altered miRNA abundance obviously provides the plant with the ability to rapidly modulate the expression of miRNA target genes in order for the plant to mount an adaptive response to environmental stress [5,63,64]. It is therefore unsurprising that miRNAs and/or their targeted genes have been demonstrated to be responsive to a range of abiotic stresses in the C_4 species, maize, sorghum, sugarcane and switchgrass [65–68].

Due to the demonstrated tolerance of *S. italica* and *S. viridis* to salt stress [1,6–9,33,34,69], combined with the phylogenetically relatedness of these two *Setaria* species to agronomically important C_4 species [27,28,38], and the ability to molecularly modify *S. viridis* as part of the continued genetic characterization of C_4 biology [42–45,70], this study profiled the salt stress responsive miRNA landscape of the shoot and root tissues of two accessions of *S. viridis* (namely, A10 and ME034V), previously demonstrated to be amenable to *Agrobacterium*-mediated transformation [42–45,70]. The cultivation of 3-day-old A10 and ME034V seedlings for a 7-day period on plant growth medium supplemented with 150 mM NaCl (salt stress) inhibited all aspects of *S. viridis* vegetative development with significant reductions documented for shoot area, fresh weight, primary root length and lateral root number. Profiling of the miRNA landscapes of 10-day-old A10 and ME034V control and salt stressed seedlings via sRNA sequencing, revealed that both the diversity and total size of the miRNA population of *S. viridis* shoot tissue was much greater than that of the root tissues. For example, 117 and 100 miRNA sRNAs were determined to be salt stress responsive in A10 and ME034V shoots respectively, versus only 60 and 58 miRNA sRNAs identified in salt stressed A10 and ME034V roots. However, the sRNA sequencing identified miRNA abundance trends for salt stressed A10 and ME034V shoot and root tissues were experimentally validated via RT-qPCR for six *S. viridis* miRNA sRNAs, including miR169, miR395, miR396, miR397, miR398 and miR408. RT-qPCR further revealed accession- and tissue-specific regulation of the expression of target genes of two miRNA regulatory modules, including the miR160/*AUXIN RESPONSE FACTOR* (*ARF*) and miR167/*ARF* regulatory modules, in the root tissues of salt stressed 10-day-old A10 and ME034V seedlings. The identification of miRNAs responsive to salt stress provides an exciting new avenue for future research into whether the molecular modification of these salt stress responsive miRNA regulatory modules provides *S. viridis* with an enhanced tolerance to salt stress.

2. Materials and Methods

2.1. Plant Material

Setaria viridis (L.) Beauv. accessions, A10 and ME034V, were used for all experimental work performed in this study due to both of these *S. viridis* accessions having been previously demonstrated to be amenable to *Agrobacterium*-mediated transformation [42–45,70]. One-year-old mature seeds were

initially dehusked and surface sterilized with a distilled water-based solution of 10% (*v*/*v*) commercial bleach and 0.1% (*v*/*v*) Tween-20 for 5 min at room temperature via gentle rotation. Seeds were then thoroughly rinsed three times with fresh changes of distilled water and via gentle hand inversion. In a biosafety cabinet, seeds were transferred to sterilized Whatman® filter paper and air dried. Using sterilized tweezers, air dried seeds were next transferred to Magenta™ tissue culture vessels that contained pre-set solid plant growth medium (1/2 strength Murashige and Skoog (MS) salts). The vessels were then transferred to a temperature-controlled plant growth cabinet (A1000 Plant Growth Chamber, Conviron®, Australia) and cultivated under a standard growth regime of 16 h of light/8 h of darkness and day/night temperatures of 22/18 °C. Three days post germination, equal numbers of A10 and ME034V seedlings were transferred under sterile conditions to new Magenta™ tissue culture vessels that contained either fresh solid MS medium (control treatment) or solid MS medium supplemented with 150 millimolar (mM) sodium chloride (NaCl) (salt stress treatment). Post transfer, the control and salt stressed A10 and ME034V seedlings were returned to the temperature-controlled growth cabinet and cultivated for an additional 7 days.

2.2. Phenotypic Assessments

Ten days post germination, representatives of A10 and ME034V seedlings were sampled from Magenta™ tissue culture vessels for photographic imaging. The (1) leaf area, (2) primary root length, and (3) number of lateral roots per primary root were determined via digital analysis of photographic images taken of 10-day-old A10 and ME034V seedlings post the 7-day control or salt stress treatment period, using ImageJ software. Post capture of the photographic images, the sampled representative seedlings were immediately used to determine the fresh weight of control and salt stressed A10 and ME034V seedlings.

2.3. Total RNA Extraction and High Throughput Sequencing of the Small RNA Fraction

Total RNA was isolated from the shoot and root tissue of four biological replicates (each biological replicate contained 4 individual plant samples) of 10-day-old control and salt stressed A10 and ME034V *S. viridis* seedlings, using TRIzol™ Reagent (Invitrogen™) according to the manufacturer's instructions. The quantity of each isolated total RNA fraction was assessed using a Nanodrop spectrophotometer (NanoDrop® ND-1000, Thermo Scientific, Australia) and, in parallel, the quality of each fraction was determined via visual assessment of an ethidium bromide-stained 1.2% (*w*/*v*) agarose gel post total RNA separation via standard electrophoresis. Five micrograms (5.0 µg) of each of the four biological replicates for each tissue type, and per treatment, were pooled together and diluted in RNase-free water to obtain a final preparation of 25 microliters (µL) of total RNA at a concentration of 800 nanograms (ng) per µL. The eight samples (including A10 control shoots, ME034V control shoots, A10 salt stress shoots, ME034V salt stress shoots, A10 control roots, ME034V control roots, A10 salt stress roots and ME034V salt stress roots) were then shipped to the Australian Genome Research Facility (AGRF; Melbourne node, Australia). The technical staff at the AGRF performed all subsequent preparatory steps prior to sequencing the small RNA fraction of the eight samples on an Illumina HiSeq 2500 platform.

2.4. Bioinformatic Profiling of the Salt Stress Responsive microRNA Landscape of Setaria viridis

Using the Qiagen CLC Genomics Workbench (11) software, sequences corresponding to those of the high throughput sequencing adapters were removed prior to performing sequence quality trimming to remove any sRNA sequencing reads that were either shorter or longer in length than the desired 15–35-nt size window. Post this initial analysis, parameters within the CLC Genomic Workbench were applied to remove any ambiguous nt at either the 5′ or 3′ terminus of each sequencing read (specifically, the removal of any 'N' nt present at sRNA termini), or to 'trim' low quality sequences using a modified 'Mott trimming' algorithm. The remaining sRNA sequences that perfectly aligned (that is, sRNA sequences that harbored zero mismatches) to known *Sorghum bicolor* miRNA sRNAs listed in miRBase release 22 [71] were then annotated. The values were next determined for: (1) the raw

read count of each detected miRNA sRNA across both treatments (control and salt); (2) the Log2 fold change in abundance for each miRNA sRNA for the salt stress treatment, compared to the control value; (3) the total number of high quality raw reads per library; and (4) the total number of miRNA sRNA raw reads per library.

2.5. Bioinformatic Identification of Setaria viridis microRNA Target Genes

To identify putative *S. viridis* target genes for miRNAs, miR160 and miR167, each respective miRNA sequence was entered into the online plant sRNA target analysis server, psRNATarget [72]. For miR160 and miR167, two *S. viridis* target genes were selected based on: (1) a low expectation score (indicative of a low number of mismatched base pairings between the mature miRNA and its putatively targeted sequence(s)); and (2) the putatively identified *S. viridis* miRNA target gene sequence returning a high degree of homology to known miR160 and miR167 target genes in either sorghum or *Arabidopsis thaliana* (*Arabidopsis*).

2.6. Quantitative Reverse Transcriptase Polymerase Chain Reaction Analysis

A quantitative reverse transcriptase polymerase chain reaction (RT-qPCR) approach was used to quantify miRNA sRNA abundance and the expression of miRNA target genes in control and salt stressed 10-day-old *S. viridis* A10 and ME034V seedlings. The same four biological replicates prepared for each of the eight samples analyzed via the high throughput sequencing approach were used for all RT-qPCR analyses reported here.

For quantification of the abundance of miRNAs, miR160, miR167, miR169, miR395, miR396, miR397, miR398 and miR408, a miRNA-specific complementary DNA (cDNA) was synthesized using 200 ng of DNase I-treated (New England BioLabs, Australia) total RNA as template and 20 units (U) of ProtoScript® II Reverse Transcriptase (New England BioLabs, Australia) according to manufacturer's instructions. The cycling conditions for miRNA-specific cDNA synthesis were 1 cycle at 16 °C for 30 min, followed by 60 cycles at 30 °C for 30 s, 42 °C for 30 s, and 50 °C for 2 s, and then by 1 cycle of 85 °C for 5 min.

To generate a high molecular weight cDNA library for the quantification of miRNA target gene expression, 5.0 µg of total RNA was treated with 5.0 U of DNase I (New England BioLabs, Australia) according to manufacturer's instructions. Post DNase I treatment, the total RNA was purified using a RNeasy Mini kit according to the manufacturer's instructions (Qiagen, Australia). One microgram (1.0 µg) of DNase I-treated, column-purified total RNA was used as the template for the synthesis of a high molecular weight cDNA library along with 20 U of ProtoScript® II Reverse Transcriptase and 2.5 µM of oligo $dT_{(18)}$, according to the manufacturer's instructions (New England Biolabs, Australia).

Each cDNA preparation was diluted to a working concentration of 50 ng/µL in RNase-free water, and 1.0 µL of working concentration cDNA was used as template in all RT-qPCR assessments. The GoTaq® qPCR Master Mix (Promega, Australia) was used as the fluorescent reagent for all RT-qPCRs performed, and all RT-qPCRs had the same cycling conditions of 1 cycle at 95 °C for 10 min, followed by 45 cycles of 95 °C for 10 s and 60 °C for 15 s. The abundance of each assessed miRNA sRNA was determined using the $2^{-\Delta\Delta CT}$ method with the small nucleolar RNA, U6, used as the internal control to normalize the relative abundance of each assessed miRNA. The expression of each identified miRNA target gene was also determined using the $2^{-\Delta\Delta CT}$ method, however the *S. viridis* reference genes, *SvASPR6* (*Sevir.3G358100*), *SvDUSP* (*Sevir.4G179200*) and *SvPP2A* (*Sevir.9G262700*) were used as the internal controls to normalize the miRNA target gene expression data with these three reference genes previously demonstrated to provide the most accurate quantification of gene expression in *S. viridis* [38]. All DNA oligonucleotides used for either miRNA-specific cDNA synthesis or the quantification of miRNA target gene expression are provided in Supplemental Table S1. All newly designed primer pairs for miRNA target gene analysis were designed using the NCBI primer-BLAST online tool. Further, the specificity of each primer pair was checked prior to their use in the reported RT-qPCR analyses via the amplification of a single amplicon of the expected size and all amplicons

were sequenced to confirm that only the targeted product had been amplified. Primer pair specificity was further confirmed via the formation of a single peak in each melt curve graph.

3. Results

3.1. Salt Stress Treatment Inhibits Setaria viridis Development

At 3 days post germination, the two *S. viridis* accessions assessed in this study, A10 and ME034V, were phenotypically indistinguishable from one another (Figure 1A,D). Furthermore, at 10 days post germination, and when cultivated under standard (control) growth conditions, both A10 and ME034V seedlings had progressed to the same stage of vegetative development with the first leaf having extended out from the coleoptile (Figure 1B,E). However, the root system of 10-day-old control grown A10 and ME034V seedlings were visually distinguishable from one another (Figure 1B,E). Specifically, visual inspection identified numerous adventitious roots formed proximal to the germinated seed in 10-day-old control grown A10 seedlings (Figure 1B), with a similar degree of adventitious root formation not observed for ME034V control seedlings (Figure 1E). However, while ME034V seedlings formed an equivalent number of lateral roots off the primary root as observed for the A10 accession, the lateral roots that formed proximal to the germinated seed of ME034V seedlings appeared to be more elongated (Figure 1E) than the lateral roots that emerged from the corresponding section of the primary root of control grown 10-day-old A10 seedlings (Figure 1B).

Figure 1C,F clearly show that the 7-day 150 mM NaCl treatment greatly inhibited all aspects of A10 and ME034V seedling development. More specifically, the total aerial tissue area of 10-day-old salt stressed A10 seedlings was determined to be 1.5 ± 0.3 mm^2, a 75.8% reduction compared to the 6.2 ± 0.6 mm^2 total aerial tissue area of control A10 seedlings of the same age (Figure 1G). An even greater degree of reduction to total aerial tissue area was observed for the ME034V accession. Namely, salt stressed 10-day-old ME034V seedlings had a total aerial tissue area of 0.9 ± 0.2 mm^2, compared to a total aerial tissue area of 6.4 ± 0.6 mm^2 for ME034V control seedlings, an 85.9% reduction (Figure 1G). Salt stress-induced inhibition of *S. viridis* development was also reflected via comparison of the fresh weights of 10-day-old control A10 (57.1 ± 9.5 mg) and ME034V (41.8 ± 8.1 mg) seedlings (Figure 1H) to that of salt stressed seedlings. More specifically, the fresh weight of salt stressed A10 (19.9 ± 4.3 mg) and ME034V (16.6 ± 2.7 mg) seedlings was reduced by 65.1 and 60.3%, respectively (Figure 1H).

Root development was also perturbed by the 7-day salt stress treatment of *S. viridis* accessions, A10 and ME034V. For example, compared to the primary root length of control 10-day-old A10 and ME034V seedlings of 6.7 ± 0.8 mm and 7.0 ± 0.9 mm respectively, primary root length was reduced by 50.7 and 45.7% in salt stressed A10 (6.7 ± 0.8 mm) and ME034V (6.7 ± 0.8 mm) seedlings of the same age (Figure 1I). Lateral root development was also determined to be inhibited by the 7-day salt stress treatment with the number of lateral roots that formed along the length of salt stressed A10 (6.1 ± 1.5) and ME034V (9.0 ± 0.8) primary roots reduced by 75.5 and 59.3% respectively, compared to their non-stressed counterparts (lateral roots per primary root; A10 = 24.9 ± 1.8 and ME034V = 22.1 ± 3.1) of the same age (Figure 1J). Interestingly, in addition to showing a much milder degree of reduction to the number of lateral roots that formed along the length of the primary root of salt stressed A10 seedlings, the lateral roots that formed from the primary root of salt stressed ME034V seedlings visually appeared to elongate to a greater length (Figure 1C,F,J). Taken together, the phenotypic analyses presented in Figure 1 clearly demonstrate that the cultivation of *S. viridis* for a 7-day period on plant growth media supplemented with 150 mM NaCl was highly detrimental to the developmental progression of this C_4 monocot grass.

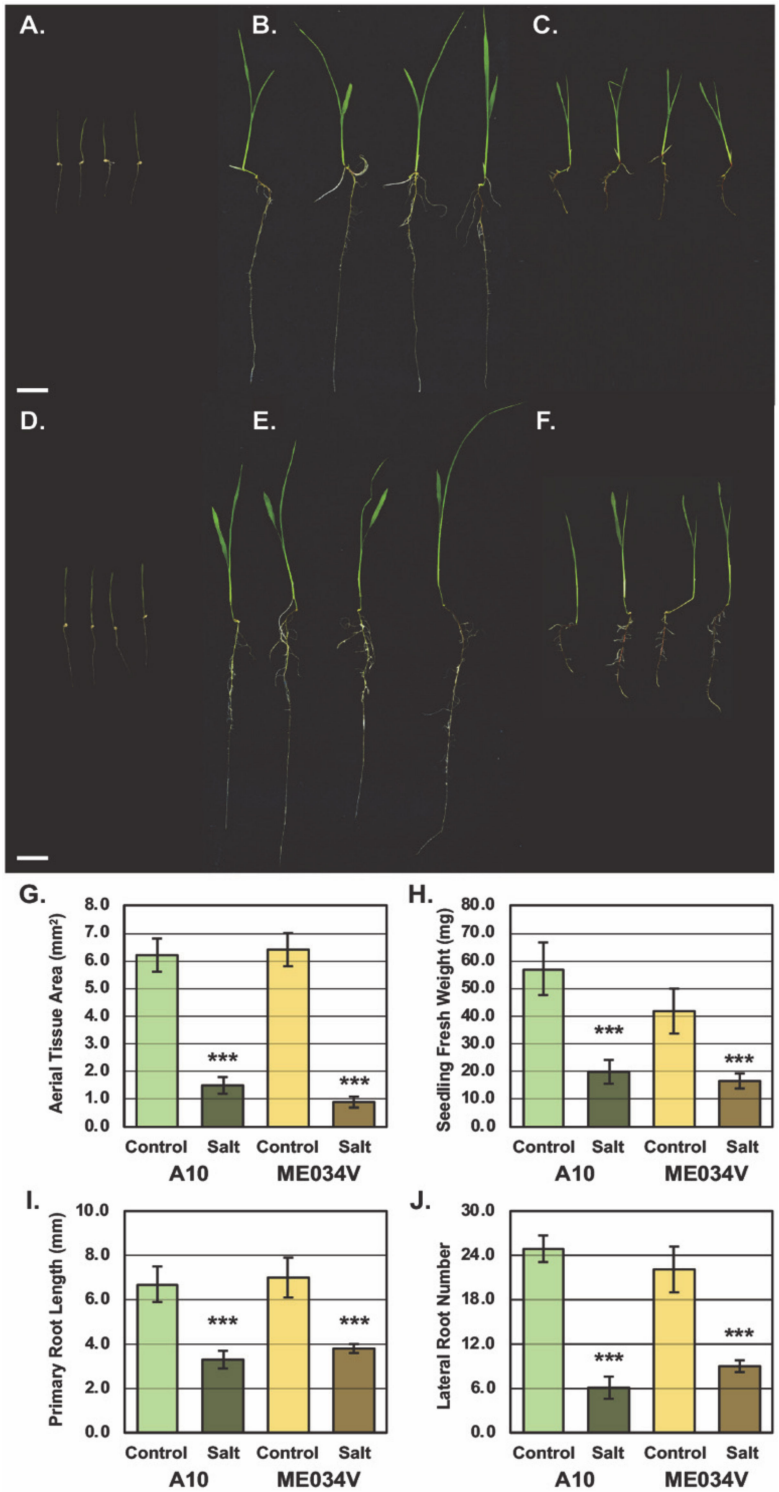

Figure 1. Assessment of the phenotypic response of *Setaria viridis* to salt stress. Phenotypes displayed by 3-day-old control (**A**), 10-day-old control (**B**), and 10-day-old salt stressed (**C**) *S. viridis* A10 seedlings. Representative phenotypes expressed by 3-day-old control (**D**), 10-day-old control (**E**), and 10-day-old salt stressed (**F**) *S. viridis* ME034V seedlings. Assessment of the phenotypic parameters, (**G**) aerial tissue area (mm^2), (**H**) seedling fresh weight (mg), (**I**) primary root length (mm), and (**J**) lateral root number, of 10-day-old control and salt stressed A10 and ME034V *S. viridis* seedlings. The bars on the histograms represent the standard deviation. Statistical data was analyzed by a *t*-test with the *p*-value indicated (*** $p < 0.001$).

3.2. Profiling of the Salt Stress Responsive MicroRNA Landscape of Setaria viridis Shoots and Roots

Having demonstrated that a 7-day cultivation period on plant growth medium supplemented with 150 mM NaCl severely inhibited the developmental progression of *S. viridis* seedlings, in combination with previous studies having identified a putative role for miRNA-directed gene expression regulation in response to this form of abiotic stress in the agronomically important monocot grass species, rice [73,74], wheat [75–77] and maize [68,78], a high throughput sRNA sequencing approach was next applied to profile the salt stress responsive miRNA landscapes of the shoot and root tissues of *S. viridis* accessions A10 and ME034V. Figure 2 clearly shows that the composition of the miRNA landscape was more diverse in the aerial tissues of *S. viridis* accessions A10 and ME034V (represented by the red and blue colored tiles in Figure 2) than in the root tissues of these two *S. viridis* accessions (represented by the white colored tiles in Figure 2). More specifically, 117 and 100 individual miRNA sRNAs were detected by the applied sRNA sequencing approach in the A10 and ME034V aerial tissue samples, respectively, versus only 60 and 58 unique miRNA sRNA reads detected via sequencing in the root tissue samples of 10-day-old A10 and ME034V seedlings (Figure 2). Supplemental Table S2 further shows that in addition to the diversity of the miRNA landscape being greater in A10 and ME034V aerial tissues than that of the root samples, the accumulation of each detected miRNA sRNA was significantly higher in A10 and ME034V shoots than in A10 and ME034V roots. For example, 780,490, 830,631, 542,794 and 560,542 miRNA sRNA reads (total = 2,714,457 sRNA sequencing reads) were detected across the control and salt stressed A10 and ME034V leaf tissue sequencing samples, versus only 17,069, 12,416, 9278 and 14,467 miRNA sRNAs (total = 53,230 sRNA sequencing reads) accumulating to levels detectable by the applied sRNA sequencing approach in control and salt stressed A10 and ME034V roots (Table S2). From Figure 2, it is also readily apparent that for the majority of miRNAs detected in A10 and ME034V shoots, and in the roots of the A10 accession, the 7-day salt stress treatment reduced the abundance of each detected sRNA. In stark contrast, the imposed salt stress treatment elevated the abundance of all but one (miR396c) of the miRNA sRNAs detected in the roots of 10-day-old ME034V seedlings (Figure 2). In addition, and of the miRNAs with elevated abundance in salt stressed A10 and ME034V leaf tissue, the abundance of all detected members of the *MIR395* gene family, including the miR395a, miR395b, miR395c, miR395d, miR395e, miR395f, miR395g, miR395h, miR395i, miR395j, miR395k and miR395l sRNAs, was elevated to the greatest degree by the imposed salt stress treatment (Figure 2), a finding that strongly suggests that the expression of all *S. viridis MIR395* genes is highly responsive to salt stress.

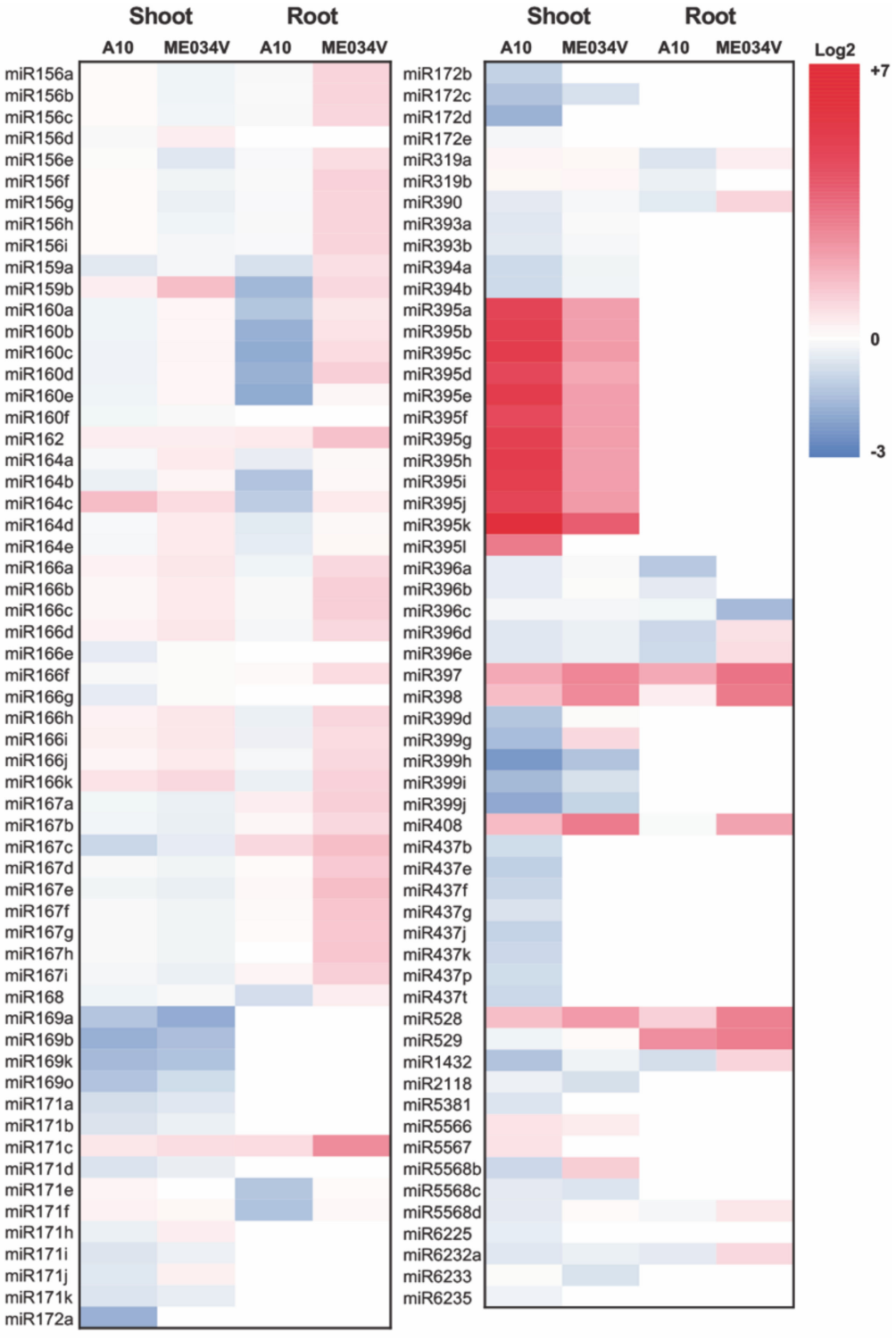

Figure 2. Profiling of the salt stress responsive microRNA landscape of the shoots and roots of 10-day-old A10 and ME034V seedlings. The four columns of the heat map depict the fold change in abundance for each miRNA detected in salt stressed A10 shoots, ME034V shoots, A10 roots and ME034V roots. Red colored tiles represent miRNAs with enhanced abundance post the 7-day salt stress treatment period while blue colored tiles depict miRNAs with reduced abundance post salt stress application. White colored tiles indicate that the miRNA failed to accumulate to detectable levels in the assessed tissue.

3.3. Experimental Validation of microRNA Abundance in Salt Stressed Setaria viridis Shoots

The sRNA sequencing approach used to profile miRNA abundance in *S. viridis* A10 and ME034V shoots revealed that the levels of numerous miRNA sRNAs were altered by the cultivation of these two *S. viridis* accessions for a 7-day period in the presence of 150 mM NaCl. A quantitative reverse transcriptase polymerase chain reaction (RT-qPCR) approach was therefore next applied to experimentally validate the sRNA sequencing identified abundance trends for miRNAs, miR169, miR395, miR396, miR397, miR398 and miR408, in control and salt stressed 10-day-old *S. viridis* A10 and ME034V shoots. It is important to note here, however, that the primers used in the RT-qPCR approach to quantify miRNA abundance do not allow for the distinction in the abundance of individual *MIR* gene family members, and therefore the reported RT-qPCR quantifications (Figures 3 and 4) represent the collective total abundance of all family members identified for each *MIR* gene family assessed.

RT-qPCR confirmed the sRNA sequencing identified trend of reduced miR169 abundance in salt stressed A10 and ME034V shoots (Figure 2; Supplemental Table S2). Namely, sequencing indicated that miR169 levels were reduced by 2.4- and 2.9-fold in salt stressed A10 and ME034V shoots respectively, compared to 10-day-old control shoots. RT-qPCR revealed that the levels of the miR169 sRNA was indeed reduced by 1.7-fold in salt stressed A10 shoots (Figure 3A), compared to control shoots. RT-qPCR additionally confirmed that miR169 abundance was significantly reduced by 2.4-fold in the shoot tissues of 10-day-old ME034V seedlings post the 7-day salt stress treatment.

Due to the sRNA sequencing approach revealing that the abundance of all detected members of the *MIR395* gene family was highly elevated in the shoot tissue of salt stressed A10 and ME034V seedlings (Figure 2; Supplemental Table S2), the level of the mature miR395 sRNA was next quantified by RT-qPCR. The abundance of the 12 *MIR395* family members detected in salt stressed A10 shoot tissue (4674 reads) was determined to be elevated by 41.7-fold compared to miR395 abundance (112 reads) in control A10 shoots (Supplemental Table S2). Although to a much lower degree, miR395 sRNA levels were confirmed to be significantly elevated by the 7-day salt stress treatment period by 2.7-fold in A10 shoots via RT-qPCR (Figure 3C). In the aerial tissues of salt stressed ME034V seedlings, sRNA sequencing recorded 1,688 reads for the 11 *MIR395* gene family members detected (Supplemental Table S2), an increase of 4.3-fold in miRNA abundance compared to the 397 reads detected in 10-day-old ME034V control shoots. The RT-qPCR approach again confirmed the sRNA sequencing data with a significant 3.4-fold elevation in miR395 abundance in salt stressed ME034V shoots demonstrated (Figure 3D). As successfully applied to the miR169 and miR395 analyses, RT-qPCR additionally confirmed the sequencing identified trend of reduced miR396 sRNA abundance in 10-day-old salt stressed A10 and ME034V seedlings compared to the respective control shoot tissues (Figure 2; Supplemental Table S2). For example, sequencing revealed miR396 levels to be reduced by 1.2- and 1.4-fold in salt stressed A10 and ME034V shoots, respectively, with this mild degree of reduction confirmed by the RT-qPCR approach, which showed miR396 abundance to be down by 1.2- and 1.4-fold in the aerial tissues of 10-day-old salt stressed A10 (Figure 3E) and ME034V seedlings (Figure 3F), respectively.

Two thousand, seven hundred and eight sequencing reads were mapped to the miR397 sRNA in the aerial tissue sample of control A10 seedlings, a read number which was determined to climb to 12,143 reads in salt stressed A10 seedlings (Supplemental Table S2). The level of the miR397 sRNA was much lower in control ME034V shoots at 123 reads, however, miR397 abundance was also induced by the 7-day salt stress treatment in the shoots of the ME034V accession, rising to 802 reads post the salt stress treatment, a 6.5-fold enhancement to miR397 sRNA abundance. RT-qPCR confirmed that miR397 levels were induced by salt stress with significant 2.1- and 2.6-fold elevations to miR397 abundance determined for 10-day-old A10 (Figure 3G) and ME034V salt stressed shoot tissues (Figure 3H), respectively.

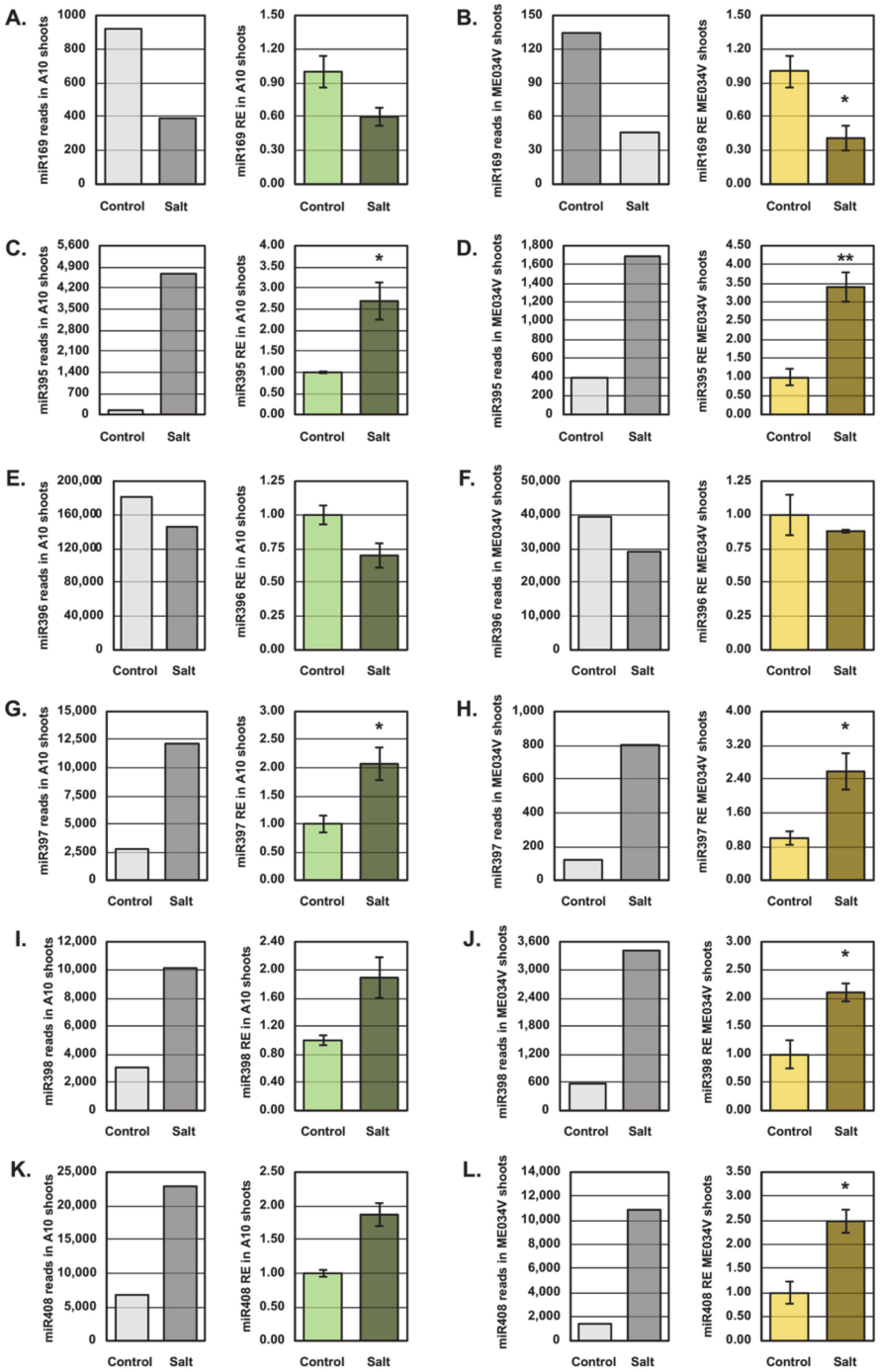

Figure 3. Experimental validation of the response of six miRNAs to salt stress in *Setaria viridis* shoots. RT-qPCR quantification of miRNA abundance to experimentally validate the sRNA sequencing identified abundance trends documented for the shoot tissue of 10-day-old salt stressed A10 and ME034V seedlings, including miR169 in salt stressed A10 (**A**) and ME034V (**B**) shoots, miR395 levels in A10 (**C**) and ME034V (**D**) salt stressed shoot tissues, miR396 abundance in salt stressed A10 (**E**) and ME034V (**F**) shoots, miR397 levels in salt stressed A10 (**G**) and ME034V (**H**) shoot material, miR398 abundance in salt stressed A10 (**I**) and ME034V (**J**) shoots, and the levels of the miR408 sRNA in salt stressed A10 (**K**) and ME034V (**L**) shoot samples. The bars on the histograms represent the standard deviation of the four biological replicates analyzed by RT-qPCR. Statistical difference was determined with a *t*-test and the asterisks representing *p*-values of * $p < 0.05$ and ** $p < 0.005$.

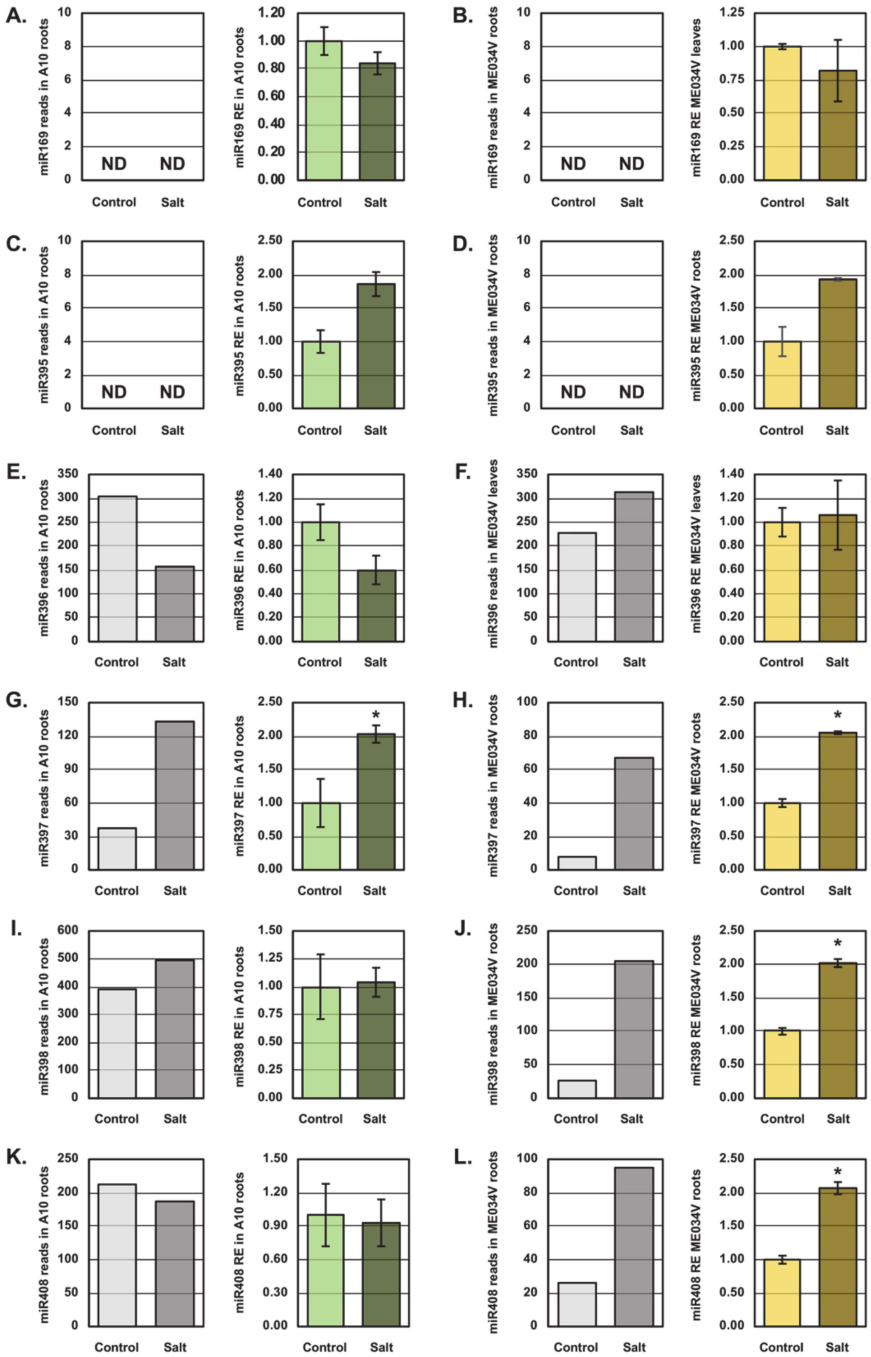

Figure 4. Experimental validation of the response of six miRNAs to salt stress in *Setaria viridis* roots. RT-qPCR quantification of miRNA abundance to experimentally validate the sRNA sequencing identified abundance trends documented for the root tissue of 10-day-old salt stressed A10 and ME034V seedlings, including miR169 in salt stressed A10 (**A**) and ME034V (**B**) roots, miR395 levels in A10 (**C**) and ME034V (**D**) salt stressed roots, miR396 abundance in salt stressed A10 (**E**) and ME034V (**F**) root tissues, miR397 levels in salt stressed A10 (**G**) and ME034V (**H**) root tissue, miR398 abundance in salt stressed A10 (**I**) and ME034V (**J**) roots, and the levels of the miR408 sRNA in salt stressed A10 (**K**) and ME034V (**L**) root tissue samples. The bars on the histograms represent the standard deviation of the four biological replicates analyzed by RT-qPCR. Statistical difference was determined with a *t*-test and the asterisk represents a *p*-value of * $p < 0.05$.

Sequencing suggested that, like miR397, miR398 abundance was induced by the salt stress treatment with 3.3- and 6.0-fold upregulated levels of the miR398 sRNA documented in salt stressed

A10 and ME034V shoots, compared to their respective controls (Figure 2; Supplemental Table S2). RT-qPCR confirmed this trend via revealing that the level of the miR398 sRNA was upregulated by 1.9-fold in salt stressed A10 shoots (Figure 3I) and significantly elevated by 2.1-fold in salt stressed ME034V aerial tissues (Figure 3J). In 10-day-old control A10 and ME034V shoots, 6,822 and 1,378 reads were mapped to the miR408 sRNA sequence. In the aerial tissues of salt stressed A10 and ME034V seedlings of the same age, 22,403 and 10,872 sequencing reads were aligned to this sRNA sequence to represent 3.4- and 7.9-fold increases in abundance, respectively (Figure 2; Supplemental Table S2). Salt stress-induced miR408 abundance was confirmed by the applied RT-qPCR approach which revealed miR408 levels to be elevated by 1.9- and 2.5-fold in salt stressed A10 (Figure 3K) and ME034V shoots (Figure 3L), compared to miR408 abundance in the aerial tissues of the respective control seedlings of the same age. Taken together, the data presented in Figure 3 shows that although the degree of miRNA abundance alteration determined via the RT-qPCR approach was lower than that identified by sRNA sequencing, RT-qPCR repeatedly confirmed the direction of the change in abundance for the six assessed miRNAs that were initially identified via sRNA sequencing as salt stress responsive miRNAs.

3.4. Experimental Validation of microRNA Abundance in Salt Stressed Setaria viridis Roots

The RT-qPCR approach was additionally applied to experimentally validate the sRNA sequencing identified abundance trends for the miR169, miR395, miR396, miR397, miR398 and miR408 sRNAs post the 7-day 150 mM NaCl stress treatment in the root tissues of *S. viridis* accessions, A10 and ME034V. In the roots of 10-day-old A10 and ME034V control and salt stressed seedlings, the sRNA sequencing approach failed to detect the miR169 and miR395 sRNAs (Figure 2; Supplemental Table S2). However, RT-qPCR revealed miR169 levels to be mildly reduced by 1.2-fold in the roots of salt stressed A10 and ME034V seedlings (Figure 4A,B) and, further, miR395 abundance to be moderately elevated by 1.9-fold (Figure 4C,D). Failure to detect miR169 and miR395 via sRNA sequencing, yet the RT-qPCR generated demonstration of reduced and elevated miR169 and miR395 abundance, respectively, indicated that RT-qPCR provided greater sensitivity for the detection of these two miRNA sRNAs in *S. viridis* root tissues. For the miR396 sRNA, both detection approaches revealed miR396 levels to be reduced in the roots of salt stressed A10 seedlings (Figure 4E). More specifically, sequencing and RT-qPCR revealed miR396 abundance to be reduced by 2.0- and 1.7-fold respectively, in salt stressed A10 roots (Figure 4E). In salt stressed root tissue of the ME034V accession, sequencing indicated that miR396 levels increased marginally to 313 reads from the 229 reads detected in control ME034V roots (Supplemental Table S2), a 1.4-fold upregulation in sRNA abundance. However, RT-qPCR indicated that the levels of this sRNA remained largely unchanged across the control and salt stress ME034V root samples (Figure 4F). The RT-qPCR assessments of miR396 abundance in salt stressed ME034V shoots (Figure 3E) and roots (Figure 4E) closely mirrored one another to suggest that the level of the miR396 sRNA was largely unaffected by the applied 7-day salt stress treatment in the ME034V accession.

In the root tissues of 10-day-old salt stressed A10 and ME034V seedlings, sRNA sequencing revealed miR397 abundance to be reduced by 3.6- and 8.4-fold, respectively. The abundance of miR397 was confirmed to be reduced by RT-qPCR, albeit to a lower degree (by 2.0-fold), in salt stressed A10 and ME034V roots (Figure 4H). The response of the miR398 sRNA to the imposed stress was demonstrated by sequencing and RT-qPCR to differ in the root systems of 10-day-old A10 and ME034V seedlings with miR398 abundance determined to remain largely unchanged in A10 salt stressed roots (Figure 4I), yet miR398 levels were significantly upregulated in ME034V salt stressed roots (Figure 4J). Similar to miR398, the miR408 sRNA differed in its response to the imposed stress with miR408 levels mildly reduced by 1.1-fold in A10 salt stressed roots (Figure 4K) and significantly elevated (sequencing, 3.7-fold up; RT-qPCR, 2.1-fold up) in salt stressed ME034V roots (Figure 4L), compared to their respective control seedlings of the same age (Figure 4K,L). For the four miRNAs (miR396, miR397, miR398 and miR408) detected by both the sRNA sequencing and RT-qPCR approach across the assessed A10 and ME034V root tissue samples, largely matching trends in abundance in response to the imposed stress

were documented, a finding which provides confidence that a biologically relevant response to salt stress was identified for each miRNA.

3.5. Molecular Assessment of the Response of the miR160 and miR167 Regulatory Modules to Salt Stress

The phenotypic data presented in Figure 1 visually shows that at 10 days post germination, the most pronounced phenotypic difference between control grown A10 and ME034V seedlings was displayed by the root system, with A10 seedlings developing adventitious roots and ME034V plants developing elongated lateral roots from the primary root zone proximal to the germinated seed. Considering that miRNAs, miR160 and miR167 (and/or their targeted genes), have been assigned roles in root development in *Arabidopsis*, tomato and maize [67,79,80], in combination with the previous demonstration that both miRNA sRNAs are responsive to salt stress in tomato, maize, *Medicago truncatula* and Black mustard (*Brassica juncea*) [68,80–82], the response of the miR160 and miR167 sRNAs, and that of two of their putative target genes, was next assessed in the shoots and roots of 10-day-old seedlings of *S. viridis* accessions, A10 and ME034V, post cultivation under standard growth conditions or the salt stress treatment.

Two putative target genes were selected as part of the analysis of the miR160 regulatory module in the A10 and ME034V *S. viridis* accessions, namely, *AUXIN RESPONSE FACTOR1* (*ARF1*; *Sevir.9G219100*) and *ARF16* (*Sevir.3G004300*). The *ARF1* gene was selected for analysis due to this putative target transcript only harboring a single nucleotide mismatch base pairing with the miR160 sRNA at the 3′ terminal nucleotide of miR160 (Figure 5A). Similarly, *ARF16* was selected as a putative target gene for analysis due to its high degree of complementarity to the miR160 sRNA (harboring a single G:U wobble pairing at nucleotide 15 from the 5′ terminal nucleotide of the miR160 sRNA) (Figure 5B), combined with *ARF16* orthologs forming known miR160 target genes in other plant species [79,83].

In the shoot tissue of control and salt stressed 10-day-old A10 seedlings, miR160 abundance remained remarkably constant with 2,504 and 2,426 reads mapped to the miR160 sRNA in control and salt stressed shoots, respectively (Supplemental Table S2). A very mild reduction in miR160 abundance in salt stressed A10 shoots was confirmed by RT-qPCR which revealed miR160 levels to be reduced 1.1-fold by the 7-day salt stress treatment (Figure 5C). RT-qPCR further revealed that in response to the mild reduction to miR160 abundance in salt stressed A10 shoots, *ARF1* and *ARF16* expression was elevated by 1.8- and 1.5-fold, respectively (Figure 5C). Elevated *ARF1* and *ARF16* abundance in salt stressed A10 shoot tissue where miR160 levels were determined to be mildly reduced is expected for a target transcript under miR160-directed expression regulation. In comparison to the aerial tissues of salt stressed A10 seedlings, miR160 abundance was determined to be reduced by a much greater degree, 3.6-fold, in salt stressed A10 roots. More specifically, sRNA sequencing identified 52 reads that mapped to the miR160 sRNA in the salt stress sample, compared to 187 sequencing reads that aligned to the miR160 sequence in A10 control roots (Supplemental Table S2). A greater degree of reduction to miR160 accumulation in salt stressed A10 roots, compared to salt stressed A10 shoots, was confirmed by RT-qPCR, which determined miR160 abundance to be reduced by 1.8-fold (Figure 5D). In response to reduced miR160 levels, *ARF1* expression was significantly increased by 3.0-fold, an expression change that strongly suggested that *ARF1* transcript abundance is indeed under miR160-directed expression regulation in both the root and shoot tissues of the *S. viridis* A10 accession. Additional evidence that the *ARF16* transcript is also a target of miR160-directed expression regulation in A10 roots could not be obtained however, with the *ARF16* transcript failing to accumulate to levels quantifiable by RT-qPCR assessment (Figure 5D).

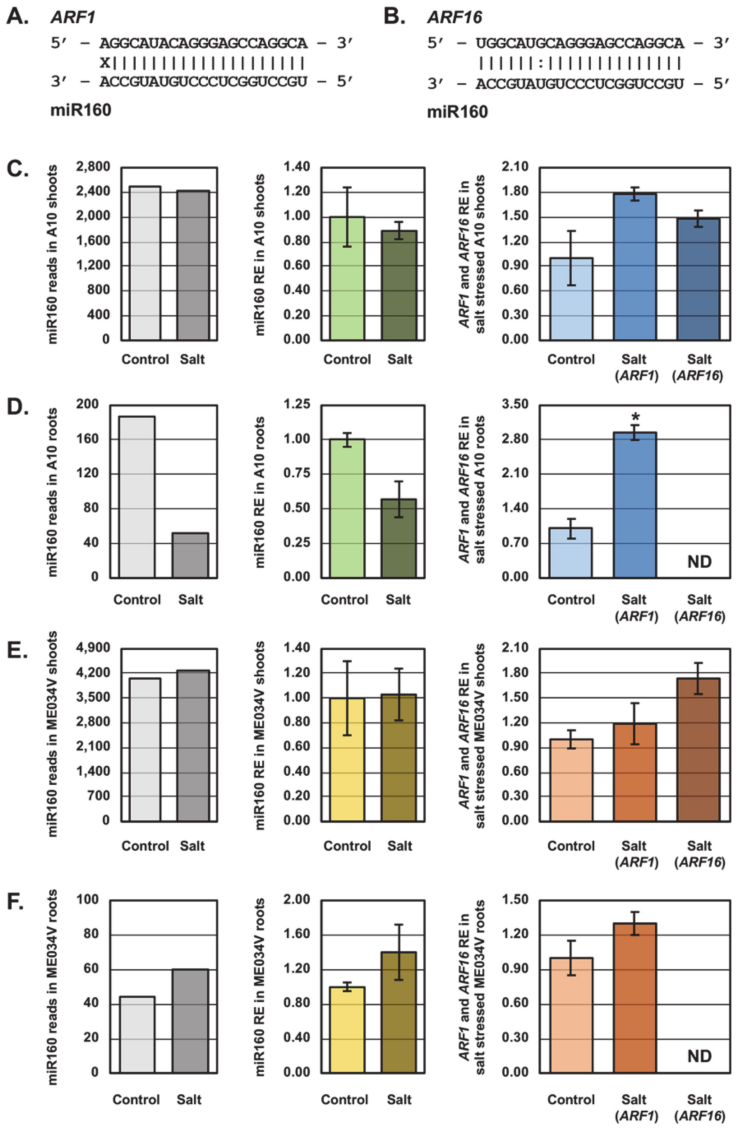

Figure 5. Molecular assessment of the response of the miR160 regulatory module to salt stress. Alignment of the *S. viridis* miR160 sRNA sequence to the putative target sequences harbored by the *S. viridis ARF1* (**A**) and *ARF16* (**B**) transcripts. RT-qPCR confirmation of the abundance of the miR160 sRNA, and the assessment of the expression of the putative miR160 target genes, *ARF1* and *ARF16*, in A10 shoot (**C**) and root (**D**) tissues in response to salt stress. Experimental validation of miR160 sRNA abundance and RT-qPCR assessment of *ARF1* and *ARF16* expression in ME034V shoots (**E**) and roots (**F**) post exposure of 10-day-old seedlings to a 7-day period of salt stress exposure. The bars on the histograms represent the standard deviation of the 4 biological replicates analyzed by RT-qPCR. Statistical differences were determined by a *t*-test with the asterisks representing the *p*-value of * $p < 0.05$.

Small RNA sequencing showed that in salt stressed ME034V shoot tissue, miR160 abundance mildly increased to 4,288 reads, from the 4,055 reads mapped to the miR160 sRNA in the ME034V control sample (Figure 5E), an approximate 1.1-fold increase in miR160 abundance. This mild increase in miR160 abundance in salt stressed ME034V shoots, compared to control ME034V shoots, was confirmed via RT-qPCR. In response to this mild elevation to miR160 levels, RT-qPCR further showed that the expression of the *ARF1* and *ARF16* target transcripts also increased (1.2- and 1.7-fold, respectively) in salt stressed ME034V shoots (Figure 5E). Elevated *ARF1* and *ARF16* expression, in parallel to documenting a mild increase to miR160 accumulation, suggested that either (1) the degree of increase in miR160 level was not significant enough to enable the miR160 sRNA to appropriately regulate

ARF1 and *ARF16* expression in response to the imposed stress; or (2) *MIR160*, *ARF1* and *ARF16* gene expression are all induced by salt stress. In the root tissue of 10-day-old salt stressed ME034V seedlings, both the sRNA sequencing and RT-qPCR approaches revealed miR160 levels to be increased by 1.4-fold (Figure 5F). RT-qPCR revealed that *ARF1* expression also increased by 1.3-fold in parallel to increased miR160 accumulation (Figure 5F). This result again indicated that in ME034V tissues, the 7-day cultivation period on plant growth medium supplemented with 150 mM NaCl mildly induced the expression of both the encoding loci of the miR160 sRNA (*MIR160* genes) and of the putative miR160 target gene, *ARF1*. As demonstrated for the A10 accession, RT-qPCR failed to detect *ARF16* expression in ME034V root tissues (Figure 5F). Failure to detect *ARF16* expression in the roots of both accessions assessed in this study (Figure 5D,F) strongly suggested that the expression of the *ARF16* gene is not localized to this *S. viridis* tissue, a suggestion that was further supported by the ready detection of *ARF16* gene expression by RT-qPCR in the aerial tissues of A10 and ME034V seedlings (Figure 5C,E).

BLAST search analysis (https://phytozome.jgi.doe.gov/pz/portal.html) of *S. viridis* transcript sequences using the *S. viridis* miR167 sRNA as the search query identified the *ARF8* (*Sevir.1G075700*) and *ARF23* (*Sevir.4G275100*) transcripts as putative miR167 targets. The *ARF8* gene (Figure 6A) was selected as a putative target of miR167-directed expression regulation primarily due to *ARF8* orthologs having been identified previously in other plant species as targets of miR167-directed expression regulation [68,80–82]. The *ARF23* transcript was included in this analysis due to this transcript forming exactly the same hybridization product with the *S. viridis* miR167 sRNA (Figure 6B) as determined for the known miR167 target gene, *ARF8*.

Figure 6C,D clearly show that for the A10 accession, neither the miR167 sRNA, nor the putative target genes, *ARF8* and *ARF23*, were responsive to the 7-day cultivation period in the presence of 150 mM NaCl. More specifically, when compared to the shoot (Figure 6C) and root (Figure 6D) tissues sampled from 10-day-old control A10 seedlings, both the sRNA sequencing and RT-qPCR approach revealed miR167 abundance to remain largely unchanged in both tissue types sampled from salt stressed A10 seedlings. RT-qPCR further revealed that in accordance with unaltered miR167 abundance, *ARF8* and *ARF23* expression showed little variation in salt stressed A10 shoots and roots, compared to the expression of both of these *ARF* genes in the A10 control samples (Figure 6C,D). In the aerial tissues of the ME034V accession however, salt stress was determined by sRNA sequencing to reduce the abundance of the miR167 sRNA by 1.3-fold (control = 34,188 reads; salt stress = 25,962 reads); a reduction that was confirmed by RT-qPCR (Figure 6E). RT-qPCR also revealed the surprise finding that *ARF8* and *ARF23* expression was reduced by 1.7- and 1.1-fold respectively (Figure 6E), in response to reduced miR167 levels in salt stressed ME034V shoots, and not elevated as would be expected for a miRNA target gene under a miRNA-directed target transcript cleavage mode of expression regulation; the mode of target gene expression regulation directed by most plant miRNAs [48,50,52]. Considering that miR167 levels were reduced in the shoots of salt stressed ME034V seedlings (Figure 6E), the 2.1- and 1.6-fold elevation in miR167 abundance, as determined via the sequencing and RT-qPCR assessment approaches respectively, of salt stressed ME034V roots (Figure 6E), was also an unexpected finding. However, the demonstration by RT-qPCR that the expression of the miR167 putative target genes, *ARF8* and *ARF23*, was reduced by 1.7- and 1.3-fold respectively in salt stressed ME034V roots (Figure 6F), provided solid evidence that elevated miR167 abundance in the roots of salt stressed ME034V seedlings formed an accurate profile of the response of this sRNA to the applied stress in the assessed tissue. Taken together, the miR160 analyses presented in Figure 5 and the miR167 assessments presented in Figure 6 show that reduced miR160 abundance and elevated *ARF1* expression was specific to the roots of salt stressed A10 seedlings (Figure 5D), whereas, elevated miR167 abundance and reduced *ARF8* expression (and to a lesser degree, reduced *ARF23* expression) was unique to the roots of salt stressed ME034V seedlings (Figure 6F).

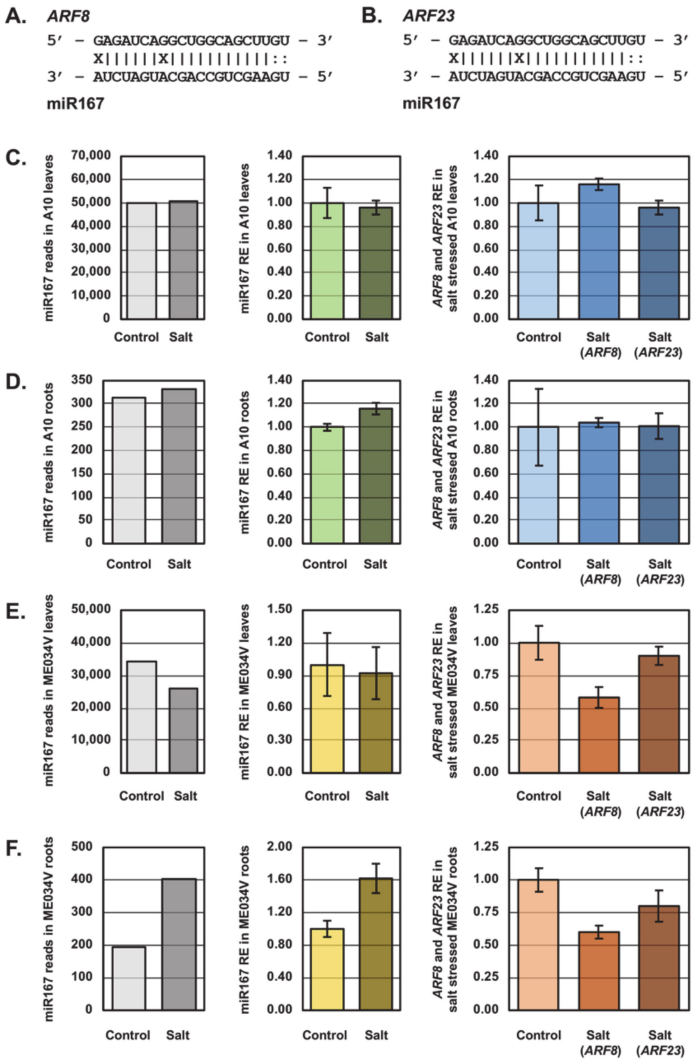

Figure 6. Molecular assessment of the response of the miR167 regulatory module to salt stress. Alignment of the *S. viridis* miR167 sRNA sequence to the putative target sequences harbored by the *S. viridis ARF8* (**A**) and *ARF23* (**B**) transcripts. Experimental validation of miR167 sRNA abundance and RT-qPCR assessment of *ARF8* and *ARF23* putative target gene expression in A10 shoots (**C**) and roots (**D**) post exposure of 10-day-old seedlings to salt stress. RT-qPCR confirmation of the abundance of the miR167 sRNA, and the assessment of the expression of the putative miR167 target genes, *ARF8* and *ARF23*, in ME034V shoot (**E**) and root (**F**) tissues in response to salt stress. The bars on the histograms represent the standard deviation of the four biological replicates analyzed. No statistical difference was identified for the assessed miR167 regulatory module transcripts.

4. Discussion

Over the last two decades, the prevalence of soil salinization has been enhanced greatly by the destructive impact of human activities, including unfavorable farming practices or the pollution generated by industry [5,10,11,13]. Therefore, soil salinization has become a compelling global agricultural problem with numerous studies demonstrating that salinity adversely impacts the yield potential of the major cereal crop species, rice, maize and wheat [2,4,11–13]. Due to the increased concentration of Na^+ and Cl^- ions in saline soils, ions that are taken up by the root system of a plant and subsequently concentrated in the aerial tissue cells, saline soils are largely unsuitable for agriculture [10,14]. Elevated levels of Na^+ and/or Cl^- ions in plant leaf cells inhibits photosynthesis and blocks carbon assimilation, both of which lead to the overall inhibition of plant growth, and ultimately plant yield [11,12,15,16]. Therefore, the initial aim of this study was to document the developmental

consequence of cultivating *S. viridis* accessions, A10 and ME034V, in a '*salt stress*' environment for a 7-day period.

Cultivation of 3-day-old *S. viridis* seedlings for a 7-day period on plant growth medium supplemented with 150 mM NaCl greatly inhibited all aspects of the development of A10 and ME034V seedlings (Figure 1). More specifically, the shoot area of salt stressed 10-day-old A10 and ME034V seedlings was reduced by 75.8 and 85.9%, respectively (Figure 1G). Significant perturbation of *S. viridis* seedling development was further demonstrated by the assessment of fresh weight following the 7-day salt stress treatment, with salt stressed A10 and ME034V seedling fresh weights reduced by 65.1 and 60.3%, respectively (Figure 1H). Root development was also severely inhibited by the imposed stress with primary root length reduced by 50.7 and 45.7% in salt stressed A10 and ME034V seedlings, respectively (Figure 1I). Lateral root development was additionally compromised by the cultivation of A10 and ME034V seedlings in the presence of 150 mM NaCl for a 7-day period (Figure 1J) with lateral root number reduced by 75.5 and 59.3%, respectively. A high degree of negative impact on *S. viridis* seedling development by the imposed salt stress treatment was not a surprise finding with this form of abiotic stress previously demonstrated to negatively impact the development of switchgrass, soybean (*Glycine max*), creeping bentgrass (*Agrostis stolonifera*) and *Arabidopsis* [84–87]. It is important to note here that, of the four phenotypic parameters reported in Figure 1, only the shoot area of salt stressed plants was decreased to a greater degree in the ME034V accession. Fresh weight, primary root length, and lateral root number were all reduced to a greater degree in salt stressed A10 seedlings. Therefore, when taken together, the Figure 1 analyses tentatively suggest that, at the phenotypic level, the ME034V accession was more tolerant than the A10 accession to the imposed, 7-day salt stress treatment.

In the agronomically important monocot grass cereals, maize, wheat and rice, a putative role for miRNA-directed gene expression regulation in response to salt stress has been previously demonstrated [73–78]. Profiling of the salt stress responsive miRNA landscapes of the shoot and root material sampled from 10-day-old A10 and ME034V seedlings was therefore undertaken in an attempt to establish a similar role for miRNA-directed gene expression in response to this form of abiotic stress in *S. viridis* seedlings. This profiling endeavor unexpectedly revealed a highly curious finding, namely, both the diversity and total population size of the miRNA landscape of *S. viridis* roots is greatly reduced in comparison to the miRNA landscape of *S. viridis* shoots (Figure 2), a finding that was repeatedly demonstrated across *S. viridis* accessions and growth conditions. For example, profiling allowed for the alignment of 1,611,121 sequencing reads to 117 miRNA sRNAs in control and salt stressed A10 shoots, and 1,103,334 reads to 100 unique miRNA sequences across both assessed ME034V aerial tissue samples (Supplemental Table S2). In stark contrast, the same profiling exercise only enabled the mapping of 29,485 sRNA sequencing reads to 60 miRNAs across the two A10 root samples, and in control and salt stressed ME034V root tissues, 58 unique miRNA sRNAs had 23,754 reads aligned to them. This unexpected result begs the question: what is the biological relevance of such a greatly reduced global miRNA population in *S. viridis* roots? This question will require the investment of significant investigative energy in the future to answer.

In order to confirm the sequencing identified trends in miRNA abundance, a standard RT-qPCR approach was employed to quantify the changes in the levels of the miR169, miR395, miR396, miR397, miR398 and miR408 sRNAs in salt stressed *S. viridis* A10 and ME034V seedlings. The abundance of miR169 was reduced in salt stressed shoot and root material sampled from 10-day-old A10 and ME034V seedlings (Figures 3 and 4). We have reported previously [3] that, in *Arabidopsis* seedlings, salt stress exposure reduced miR169 accumulation. Reduced miR169 abundance in *S. viridis* (Figures 3 and 4) and *Arabidopsis* seedlings [3] opposes the miR169 abundance trends reported for salt stressed rice and cotton (*Gossypium hirsutum*) plants [88,89]. The opposing abundance trends for the miR169 sRNA post exposure of *S. viridis* (Figures 3 and 4), *Arabidopsis* [3], rice [88] and cotton [89] to salt stress is most likely due to the unique *cis*-regulatory element landscape of the promoter regions of the *MIR169* genes encoded by each plant species [5]. In the aerial tissues of salt stressed A10 and ME034V seedlings, sRNA sequencing readily revealed a highly altered accumulation profile for miR395

(Figure 2; Supplemental Table S2). Significantly elevated miR395 abundance in salt stressed A10 and MV034V shoots was confirmed by RT-qPCR (Figure 3C,D). RT-qPCR additionally revealed elevated miR395 levels in the root tissues sampled from salt stressed A10 and ME034V seedlings (Figure 4C,D). Interestingly, in canola (*Brassica napus*) and cotton, miR395 levels have been demonstrated to be reduced by salt stress exposure [90,91], and not elevated as documented here. Again, the difference in the response of the miR395 sRNA to salt stress in *S. viridis*, canola [90] and cotton [91], is most likely due to the individual *cis*-regulatory elements harbored by the regulatory regions (primarily the gene promoter regions) of *MIR395* gene family members of each of these plant species [5].

RT-qPCR additionally confirmed the reduced abundance of the miR396 sRNA for the salt stressed A10 and ME034V shoot samples (Figure 3E,F), and the A10 salt stressed root sample (Figure 4E). Interestingly, miR396 abundance was experimentally validated by the RT-qPCR approach to be marginally elevated in salt stressed ME034V roots (Figure 4F). In molecularly modified creeping bentgrass, [81], the overexpression of a miR396 encoding sequence from rice (*Os-MIR396C*), provided the generated creeping bentgrass transformant lines with an enhanced degree of tolerance to salt stress. Considering that *S. viridis* is amenable to molecular manipulation via *Agrobacterium*-mediated transformation [43–46,70], a highly interesting research endeavor of a future study would be to determine if the overexpression of a *S. viridis* encoded miR396 precursor transcript in either the A10 or ME034V accession would similarly confer the generated *S. viridis* transformant lines with an enhanced degree of tolerance to salt stress. Elevated miR397 abundance was also experimentally validated by RT-qPCR across the shoot (Figure 3G,H) and root (Figure 4G,H) tissues of 10-day-old A10 and ME034V seedlings. In salt stressed wheat seedlings, [76], miR397 levels were reduced, a finding that again differs from the molecular response of the *S. viridis* miR397 sRNA to salt stress reported here.

In the shoot (Figure 3) and root tissues (Figure 4) of salt stressed A10 and ME034V seedlings, sRNA sequencing revealed miR398 abundance to be elevated, an abundance alteration which was readily confirmed via RT-qPCR quantification of miR398 levels. Elevated levels of the miR398 sRNA in response to the imposed salt stress in *S. viridis* shoot and root tissues is a curious result in the context of previous research that demonstrates that, in order to provide protection to plant cells against the oxidative damage that stems from the various forms of abiotic stress, miR398 abundance is reduced [89]. Reduced miR398 abundance, in turn, leads to the increased abundance of the protein products of its *COPPER/ZINC SUPEROXIDE DISMUTASE* (*CSD*) target genes, *CSD1* and *CSD2* [89]. The observed elevation to miR398 abundance in salt stressed *S. viridis* seedlings may be the result of the miR398 sRNA scaling with the abundance of its target gene transcripts, *CSD1* and *CSD2*, to attempt to fine tune the levels of the CSD1 and CSD2 target proteins in salt stressed *S. viridis* cells. Alternatively, in *S. viridis*, *MIR398* gene expression, along with the expression of the miR398 target genes, *CSD1* and *CSD2*, are all potentially induced in response to salt stress. However, analysis of the expression of *CSD1* and *CSD2*, and of *MIR398* gene family members, to determine if their abundance was elevated in parallel with the documented miR398 abundance elevation, was not conducted as part of the experimentation performed in the present study. In the aerial tissues of A10 seedlings, and shoots and roots of ME034V plants, sRNA sequencing and RT-qPCR revealed that miR408 abundance was elevated by the 7-day salt stress treatment (Figures 3 and 4). Elevated miR408 abundance has been previously reported for salt stressed *Salvia miltiorrhiza* plants, a widely used medicinal plant in traditional Chinese medicine [92]. Furthermore, [92] went on to demonstrate that the overexpression of the *S. miltiorrhiza* miR408 precursor transcript in molecularly modified tobacco provided the modified tobacco lines with an enhanced tolerance to salt stress. Therefore, enhanced miR408 levels in salt stressed A10 shoots and ME034V shoots and roots potentially functions in an analogous manner to the *S. miltiorrhiza* miR408 sRNA to direct the molecular responses required by *S. viridis* to respond to salt stress. Curiously, sRNA sequencing and RT-qPCR showed an opposing abundance trend for the miR408 sRNA in salt stressed A10 roots (Figure 4K), compared to its enhanced abundance in salt stressed A10 shoots (Figure 3K), ME034V shoots (Figure 3L) and roots (Figure 4L). Decreased miR408 levels have been reported previously in rice in response to salt stress [92], a finding that adds significant support to the

view that reduced miR408 levels in salt stressed A10 roots is a biological relevant molecular response to salt stress exposure in this specific tissue of the *S. viridis* A10 accession. When taken together, the experimental validation by RT-qPCR of the sRNA sequencing identified alterations to miRNA (miR169, miR395, miR396, miR397, miR398 and miR408) abundance in salt stressed A10 and ME034V shoots (Figure 3) and roots (Figure 4), confirmed the suitability of the application of either of these technologies to generate an accurate molecular profile of the miRNA landscape of both *S. viridis* accessions, across different tissue types, and under altered growth environments.

Assessment of the miR160 regulatory module in the *S. viridis* A10 and ME034V accessions revealed some interesting results (Figure 5). Namely, in salt stressed A10 shoots and roots, miR160 abundance was confirmed by RT-qPCR to be reduced by 11 and 43%, respectively (Figure 5C,D). Accordingly, *ARF1* and *ARF16* expression was determined to be elevated by 1.8- and 1.5-fold in salt stressed A10 shoots, and for *ARF1* expression to be elevated by 3.0-fold in A10 roots. In salt stressed ME034V shoots and roots however, miR160 levels were determined by RT-qPCR to remain largely unchanged (upregulated by 3%), and to be elevated by 40%, respectively. Surprisingly, RT-qPCR revealed *ARF1* expression to also be elevated in salt stressed ME034V shoots (Figure 5E) and roots (Figure 5F), and for the abundance of the *ARF16* transcript to also increase in ME034V shoots (Figure 5E). For *ARF* target genes under a miR160-directed transcript cleavage mode of expression regulation, elevated miR160 levels would be expected to result in decreased target transcript expression. Therefore, enhanced *ARF1* and *ARF16* expression in ME034V shoots and roots, in parallel with elevated miR160 levels, either suggests that: (1) these two *ARF* transcripts are regulated via a miR160-directed translational repression mode of target gene expression regulation in ME034V tissues; or (2) the expression of the *MIR160* loci, together with the *ARF1* and *ARF16* target genes, is induced by the imposed stress due to the promoter regions of these loci sharing similar *cis*-regulatory element compositions. As documented for miR160 in salt stressed A10 roots, miR160 abundance is reduced by salt stress exposure of *M. truncatula* and Black mustard [81,82]. Furthermore, the *ARF1* transcript identified here as a putative miR160 target gene displays a high degree of homology to the known miR160 target gene, *ARF17*, in other plant species (data not shown). In *Arabidopsis*, elevated ARF17 abundance due to reduced levels of the targeting miRNA, miR160, or via the molecular release of the *ARF17* transcript from miR160-directed expression regulation, has been demonstrated to repress lateral root formation and to promote adventitious root development [79,83], with adventitious root development in the A10 accession (Figure 1B,C), forming a clear phenotypic distinction from ME034V seedlings at the same stage of vegetative development (Figure 1E,F).

Molecular profiling of the miR167 regulatory module in 10-day-old *S. viridis* A10 and ME034V seedlings generated distinct profiles for the root tissues of these two accessions (Figure 6). Compared to control A10 seedlings, miR167 abundance and *ARF8* and *ARF23* expression only showed very mild alterations in the shoot and root tissues of salt stressed A10 seedlings (Figure 6C,D). RT-qPCR further revealed only a mild 1.1-fold reduction to miR160 abundance in salt stressed ME034V shoots (Figure 6E). In spite of this mild reduction to the level of the miR167 sRNA in ME034V shoot tissue post the 7-day salt stress treatment, RT-qPCR unexpectedly revealed *ARF8* expression to be reduced by 42% (Figure 6E). A similar degree of *ARF8* expression reduction, 40%, was observed in salt stressed ME034V roots (Figure 6F). However, in this tissue, miR167 levels were elevated by 1.6-fold; a finding that indeed suggests that in the root tissues of the *S. viridis* ME034V accession, the expression of *ARF8* is regulated via a miR167-directed transcript cleavage mode of expression regulation. In salt stressed maize [68] and tomato [80], miR167 levels have been reported to be reduced, and not elevated as documented here for salt stressed A10 and ME034V roots (Figure 6D,F). Previous research [67,83], has shown that reduced miR167 levels in the roots of *Arabidopsis* and maize, promotes adventitious root formation via the activity of ARF8 (in conjunction with ARF6). Therefore, the elevated miR167 abundance documented here, leading to reduced *ARF8* expression in salt stressed ME034V roots (and therefore reduced ARF8 protein abundance), could, in part, explain why in this accession of *S. viridis*, adventitious root formation was not pronounced, while the formation of lateral roots appeared

to be promoted. Together, the molecular profiling of the miR160 and miR167 regulatory modules in the shoot and root tissues of A10 and ME034V seedlings clearly demonstrated that the regulatory mechanisms of these two miRNA-directed modules are highly distinct from one another, even across two very closely related *S. viridis* accessions.

5. Conclusions

Considering that soil salinization is now a major (and ever growing) agricultural problem globally, obtainment of a more detailed understanding of the complex and interrelated molecular pathways that drive the biochemical, physiological and phenotypic responses of a plant to adapt to growth in a '*salty*' environment is more significant than it has ever been before. The ability to molecularly modify *S. viridis* via an *Agrobacterium*-mediated transformation approach has opened a new avenue for the further genetic characterization of the C_4 monocot grasses, with the C_4 species of monocot grass encompassing the agriculturally important cropping species, maize, sorghum and sugarcane. Across a wide range of plant species, and in addition to their well-documented role as crucial regulators of plant developmental gene expression, miRNAs play a key regulatory role at the molecular level in the adaptive responses of plants to abiotic stress, including their exposure to salt stress. Therefore, the identification of *S. viridis* miRNA regulatory modules responsive to salt stress, which can be molecularly manipulated in this species to determine whether such modification provides the generated plant lines with an enhanced tolerance to this stress, forms a crucial first step in the future genetic improvement of the C_4 monocot grasses for their continued use in agriculture in an attempt to maintain future yields in an increasingly unfavorable growth environment.

Supplementary Materials: The following are available online at http://www.mdpi.com/2073-4395/10/6/837/s1, Table S1: Sequences of DNA oligonucleotides used in this study. Table S2: microRNA read number for each detected *S. viridis* microRNA in A10 and ME034V seedlings.

Author Contributions: C.P.L.G., and A.L.E., conceived and designed the research; J.L.P., and D.Q.N., performed the experiments and analyzed the data; J.L.P., D.Q.N., C.P.L.G., and A.L.E., authored the manuscript, and; J.L.P., D.Q.N., C.P.L.G., and A.L.E., have read and agreed to the published version of the manuscript.

Funding: This research received no external funding.

Acknowledgments: The authors would like to thank fellow members of the Centre for Plant Science at the University of Newcastle for their guidance with plant growth care.

Conflicts of Interest: The authors declare no conflict of interest.

References

1. Chanwala, J.; Satpati, S.; Dixit, A.; Parida, A.; Giri, M.K.; Dey, N. Genome-wide identification and expression analysis of WRKY transcription factors in pearl millet (*Pennisetum glaucum*) under dehydration and salinity stress. *BMC Genomics* **2020**, *21*, 231. [CrossRef] [PubMed]
2. Pandey, K.; Lahiani, M.H.; Hicks, V.K.; Hudson, M.K.; Green, M.J.; Khodakovskaya, M. Effects of carbon-based nanomaterials on seed germination, biomass accumulation and salt stress response of bioenergy crops. *PLoS ONE* **2018**, *13*, e0202274. [CrossRef] [PubMed]
3. Pegler, J.L.; Oultram, J.M.J.; Grof, C.P.L.; Eamens, A.L. Profiling the abiotic stress responsive microRNA landscape of *Arabidopsis thaliana*. *Plants* **2019**, *8*, 58. [CrossRef] [PubMed]
4. Manoj, V.M.; Anunanthini, P.; Swathik, P.C.; Dharshini, S.; Ashwin Narayan, J.; Manickavasagam, M.; Sathishkumar, R.; Suresha, G.S.; Hemaprabha, G.; Ram, B.; et al. Comparative analysis of glyoxalase pathway genes in *Erianthus arundinaceus* and commercial sugarcane hybrid under salinity and drought conditions. *BMC Genomics* **2019**, *19*, 986. [CrossRef]
5. Pegler, J.L.; Grof, C.P.L.; Eamens, A.L. Profiling of the differential abundance of drought and salt stress-responsive microRNAs across grass crop and genetic model plant species. *Agronomy* **2018**, *8*, 118. [CrossRef]
6. Pan, Y.; Li, J.; Jiao, L.; Li, C.; Zhu, D.; Yu, J. A non-specific *Setaria italica* lipid transfer protein gene plays a critical role under abiotic stress. *Front. Plant Sci.* **2016**, *7*, 1752. [CrossRef]

7. Lata, C.; Mishra, A.K.; Muthamilarasan, M.; Bonthala, V.S.; Khan, Y.; Prasad, M. Genome-wide investigation and expression profiling of AP2/ERF transcription factor superfamily in foxtail millet (*Setaria italica* L.). *PLoS ONE* **2014**, *9*, e113092. [CrossRef]
8. Li, C.; Yue, J.; Wu, X.; Xu, C.; Yu, J. An ABA-responsive DRE-binding protein gene from *Setaria italica*, SiARDP, the target gene of SiAREB, plays a critical role under drought stress. *J. Exp. Bot.* **2014**, *65*, 5415–5427. [CrossRef]
9. Li, J.; Dong, Y.; Li, C.; Pan, Y.; Yu, J. *SiASR4*, the target gene of SiARDP from *Setaria italica*, improves abiotic stress adaption in plants. *Front. Plant Sci.* **2017**, *7*, 2053. [CrossRef]
10. Pandey, G.; Yadav, C.B.; Sahu, P.P.; Muthamilarasan, M.; Prasad, M. Salinity induced differential methylation patterns in contrasting cultivars of foxtail millet (*Setaria italica* L.). *Plant Cell Rep.* **2017**, *36*, 759–772. [CrossRef]
11. Puranik, S.; Bahadur, R.P.; Srivastava, P.S.; Prasad, M. Molecular cloning and characterization of a membrane associated NAC family gene, SiNAC from foxtail millet (*Setaria italica* (L.) P. Beauv). *Mol. Biotechnol.* **2011**, *49*, 138–150. [CrossRef]
12. Yang, Z.; Chi, X.; Guo, F.; Jin, X.; Luo, H.; Hawar, A.; Chen, Y.; Feng, K.; Wang, B.; Qi, J.; et al. SbWRKY30 enhances the drought tolerance of plants and regulates a drought stress-responsive gene, SbRD19, in sorghum. *J. Plant Physiol.* **2020**, *246–247*, 153142. [CrossRef] [PubMed]
13. Chen, M.; Yang, Z.; Liu, J.; Zhu, T.; Wei, X.; Fan, H.; Wang, B. Adaptation mechanism of salt excluders under saline conditions and its applications. *Int. J. Mol. Sci.* **2018**, *19*, E3668. [CrossRef] [PubMed]
14. Mickelbart, M.V.; Hasegawa, P.M.; Bailey-Serres, J. Genetic mechanisms of abiotic stress tolerance that translate to crop yield stability. *Nat. Rev. Genet.* **2015**, *16*, 237–251. [CrossRef] [PubMed]
15. Feng, Z.T.; Deng, Y.Q.; Fan, H.; Sun, Q.J.; Sui, N.; Wang, B.S. Effects of NaCl stress on the growth and photosynthetic characteristics of *Ulmus pumila* L. seedlings in sand culture. *Photosynthetica* **2014**, *52*, 313–320. [CrossRef]
16. Hasegawa, P.M.; Bressan, R.A.; Zhu, J.K.; Bohnert, H.J. Plant cellular and molecular responses to high salinity. *Annu. Rev. Plant Physiol. Plant Mol. Biol.* **2000**, *51*, 463–499. [CrossRef] [PubMed]
17. Sudhir, P.; Murthy, S.D.S. Effects of salt stress on basic processes of photosynthesis. *Photosynthetica* **2004**, *42*, 481–486. [CrossRef]
18. Wydrzynski, T.J. Water splitting by Photosystem II—where do we go from here? *Photosynthesis Res.* **2008**, *98*, 43–51. [CrossRef]
19. Ma, Q.; Yue, L.J.; Zhang, J.L.; Wu, G.Q.; Bao, A.K.; Wang, S.M. Sodium chloride improves photosynthesis and water status in the succulent xerophyte *Zygophyllum xanthoxylum*. *Tree Physiol.* **2012**, *32*, 4–13. [CrossRef]
20. Song, J.; Zhou, J.; Zhao, W.; Xu, H.; Wang, F.; Xu, Y.; Wang, L.; Tian, C. Effects of salinity and nitrate on production and germination of dimorphic seeds applied both through the mother plant and exogenously during germination in *Suaeda salsa*. *Plant Species Biol.* **2016**, *31*, 19–28. [CrossRef]
21. Sui, N.; Han, G. Salt-induced photoinhibition of PSII is alleviated in halophyte *Thellungiella halophila* by increases of unsaturated fatty acids in membrane lipids. *Acta Physiologiae Plantarum* **2014**, *36*, 983–992. [CrossRef]
22. Sui, N.; Li, M.; Li, K.; Song, J.; Wang, B.S. Increase in unsaturated fatty acids in membrane lipids of *Suaeda salsa* L. enhances protection of photosystem II under high salinity. *Photosynthetica* **2010**, *48*, 623–629. [CrossRef]
23. Sui, N.; Yang, Z.; Liu, M.; Wang, B. Identification and transcriptomic profiling of genes involved in increasing sugar content during salt stress in sweet sorghum leaves. *BMC Genomics* **2015**, *16*, 534. [CrossRef] [PubMed]
24. Foley, J.A.; Ramankutty, N.; Brauman, K.A.; Cassidy, E.S.; Gerber, J.S.; Johnston, M.; Mueller, N.D.; O'Connell, C.; Ray, D.K.; West, P.C.; et al. Solutions for a cultivated plant. *Nature* **2011**, *478*, 337–342. [CrossRef]
25. Glover, J.D.; Reganold, J.P.; Bell, L.W.; Borevitz, J.; Brummer, E.C.; Buckler, E.S.; Cox, C.M.; Cox, T.S.; Crews, T.E.; Culman, S.W.; et al. Agriculture. Increased food and ecosystem security via perennial grains. *Science* **2010**, *328*, 1638–1639. [CrossRef] [PubMed]
26. Sarwar, M.H.; Sarwar, M.F.; Sarwar, M.; Qadri, N.A.; Moghal, S. The importance of cereals (Poaceae: Gramineae) nutrition in human health: A review. *J. Cereals Oilseeds* **2013**, *4*, 32–35. [CrossRef]
27. Li, P.; Brutnell, T.P. *Setaria viridis* and *Setaria italica*, model genetic systems for the Panicoid grasses. *J. Exp. Bot.* **2011**, *62*, 3031–3037. [CrossRef]
28. Brutnell, T.P.; Wang, L.; Swartwood, K.; Goldschmidt, A.; Jackson, D.; Zhu, X.G.; Kellogg, E.; Van Eck, J. *Setaria viridis*: a model for C4 photosynthesis. *Plant Cell* **2010**, *22*, 2537–2544. [CrossRef]

29. Sebastian, J.; Wong, M.K.; Tang, E.; Dinneny, J.R. Methods to promote germination of dormant *Setaria viridis* seeds. *PLoS ONE* **2014**, *9*, e0095109. [CrossRef]
30. Mullet, J.; Morishige, D.; McCormick, R.; Truong, S.; Hilley, J.; McKinley, B.; Anderson, R.; Olson, S.N.; Rooney, W. Energy sorghum–a genetic model for the design of C_4 grass bioenergy crops. *J. Exp. Bot.* **2014**, *65*, 3479–3489. [CrossRef]
31. Hoang, N.V.; Furtado, A.; Botha, F.C.; Simmons, B.A.; Henry, R.J. Potential for genetic improvement of sugarcane as a source of biomass for biofuels. *Front. Bioeng. Biotechnol.* **2015**, *3*, 182. [CrossRef]
32. Osbourne, C.P.; Beerling, D.J. Nature's green revolution: the remarkable evolutionary rise of C_4 plants. *Philos Trans R Soc. Lond. B Biol. Sci.* **2006**, *361*, 173–194. [CrossRef] [PubMed]
33. Barton, L.; Newsome, S.D.; Chen, F.H.; Wang, H.; Guilderson, T.P.; Bettinger, R.L. Agricultural origins and the isotopic identity of domestication in northern China. *Proc. Natl. Acad. Sci. USA* **2009**, *106*, 5523–5528. [CrossRef] [PubMed]
34. Bettinger, R.L.; Barton, L.; Morgan, C. The origins of food production in north China: A different kind of agricultural revolution. *Evolutionary Anthropology* **2010**, *19*, 9–21. [CrossRef]
35. Doust, A.N.; Kellogg, E.A.; Devos, K.M.; Bennetzen, J.L. Foxtail millet: A sequence-driven grass model system. *Plant Physiol.* **2009**, *149*, 137–141. [CrossRef] [PubMed]
36. Zhang, H.; Xiao, W.; Yu, W.; Yao, L.; Li, L.; Wei, J.; Li, R. Foxtail millet SiHAK1 excites extreme high-affinity K^+ uptake to maintain K^+ homeostasis under low K^+ or salt stress. *Plant Cell Rep.* **2018**, *37*, 1533–1546. [CrossRef]
37. Diao, X.M.; Schnable, J.; Bennetzen, J.L.; Li, J. Initiation of *Setaria* as a model plant. *Front. Agric. Sci. Eng.* **2014**, *1*, 16–20.
38. Nguyen, D.Q.; Eamens, A.L.; Grof, C.P.L. Reference gene identification for reliable normalisation of quantitative RT-PCR data in *Setaria viridis*. *Plant Methods* **2018**, *14*, 24. [CrossRef]
39. Bennetzen, J.L.; Schmutz, J.; Wang, H.; Percifield, R.; Hawkins, J.; Pontaroli, A.C.; Estep, M.; Feng, L.; Vaughn, J.N.; Grimwood, J.; et al. Reference genome sequence of the model plant *Setaria*. *Nat. Biotechnol.* **2012**, *30*, 555–561. [CrossRef]
40. Martin, A.P.; Palmer, W.M.; Byrt, C.S.; Furbank, R.T.; Grof, C.P. A holistic high-throughput screening framework for biofuel feedstock assessment that characterises variations in soluble sugars and cell wall composition in *Sorghum bicolor*. *Biotechnol. Biofuels* **2013**, *6*, 186. [CrossRef]
41. Studer, A.J.; Schnable, J.C.; Weissmann, S.; Kolbe, A.R.; McKain, M.R.; Shao, Y.; Cousins, A.B.; Kellogg, E.A.; Brutnell, T.P. The draft genome of the C_3 panicoid grass species *Dichanthelium oligosanthes*. *Genome Biol.* **2016**, *17*, 223–241. [CrossRef]
42. Martins, P.K.; Nakayama, T.J.; Ribeiro, A.P.; Cunha, B.; Nepomuceno, A.L.; Harmon, F.G.; Kobayashi, A.K.; Molinari, H.B.C. *Setaria viridis* floral-dip: a simple and rapid *Agrobacterium*-mediated transformation method. *Biotechnol. Rep.* **2015**, *6*, 61–63. [CrossRef] [PubMed]
43. Martins, P.K.; Ribeiro, A.P.; Cunha, B.; Kobayashi, A.K.; Molinari, H.B.C. A simple and highly efficient *Agrobacterium*-mediated transformation protocol for *Setaria viridis*. *Biotechnol. Rep.* **2015**, *6*, 41–44. [CrossRef]
44. Van Eck, J.; Swartwood, K. *Setaria viridis*; Springer: New York, NY, USA, 2015; Volume 1223, pp. 57–67. [PubMed]
45. Nguyen, D.Q.; Van Eck, J.; Eamens, A.L.; Grof, C.P.L. Robust and reproducible *Agrobacterium*-mediated transformation system of the C_4 genetic model species *Setaria viridis*. *Front. Plant Sci.* **2020**, *11*, 281. [CrossRef]
46. Baulcombe, D.C. RNA silencing in plants. *Nature* **2004**, *431*, 356–363. [CrossRef] [PubMed]
47. Reinhart, B.J.; Weinstein, E.G.; Rhoades, M.W.; Bartel, B.; Bartel, D.P. MicroRNAs in plants. *Genes Dev.* **2002**, *16*, 1616–1626. [CrossRef] [PubMed]
48. Vazquez, F.; Gasciolli, V.; Crété, P.; Vaucheret, H. The nuclear dsRNA binding protein HYL1 is required for microRNA accumulation and plant development, but not posttranscriptional transgene silencing. *Curr. Biol.* **2004**, *14*, 346–351. [CrossRef] [PubMed]
49. Bartel, D.P. MicroRNAs: Genomics, biogenesis, mechanism, and function. *Cell* **2004**, *116*, 281–297. [CrossRef]
50. Kurihara, Y.; Takashi, Y.; Watanabe, Y. The interaction between DCL1 and HYL1 is important for efficient and precise processing of pri-miRNA in plant microRNA biogenesis. *RNA* **2006**, *12*, 206–212. [CrossRef]
51. Pegler, J.L.; Grof, C.P.L.; Eamens, A.L. The plant microRNA pathway: The production and action stages. *Methods Mol. Biol.* **2019**, *1932*, 15–39.

52. Baumberger, N.; Baulcombe, D.C. *Arabidopsis* ARGONAUTE1 is an RNA Slicer that selectively recruits microRNAs and short interfering RNAs. *Proc. Natl. Acad. Sci. USA* **2005**, *102*, 11928–11933. [CrossRef]
53. Chen, X. A microRNA as a translational repressor of APETALA2 in *Arabidopsis* flower development. *Science* **2004**, *303*, 2022–2025. [CrossRef]
54. Reis, R.S.; Hart-Smith, G.; Eamens, A.L.; Wilkins, M.R.; Waterhouse, P.M. Gene regulation by translational inhibition is determined by Dicer partnering proteins. *Nat. Plants* **2015**, *1*, 14027. [CrossRef]
55. Palatnik, J.F.; Allen, E.; Wu, X.; Schommer, C.; Schwab, R.; Carrington, J.C.; Weigel, D. Control of leaf morphogenesis by microRNAs. *Nature* **2003**, *425*, 257–263. [CrossRef]
56. Kasschau, K.D.; Xie, Z.; Allen, E.; Llave, C.; Chapman, E.J.; Krizan, K.A.; Carrington, J.C. P1/HC-Pro, a viral suppressor of RNA silencing, interferes with *Arabidopsis* development and miRNA function. *Dev. Cell* **2003**, *4*, 205–217. [CrossRef]
57. Shen, W.X.; Au, P.C.; Shi, B.J.; Smith, N.A.; Dennis, E.S.; Guo, H.S.; Zhou, C.Y.; Wang, M.B. Satellite RNAs interfere with the function of viral RNA silencing suppressors. *Front. Plant Sci.* **2015**, *6*, 281. [CrossRef]
58. Kumar, R. Role of microRNAs in biotic and abiotic stress responses in crop plants. *Appl. Biochem. Biotechnol.* **2014**, *174*, 93–115. [CrossRef]
59. Khraiwesh, B.; Zhu, J.K.; Zhu, J. Role of miRNAs and siRNAs in biotic and abiotic stress responses of plants. *BBA Gene Regul. Mech.* **2012**, *1819*, 137–148. [CrossRef]
60. Liu, H.H.; Tian, X.; Li, Y.J.; Wu, C.A.; Zheng, C.C. Microarray-based analysis of stress-regulated microRNAs in *Arabidopsis thaliana*. *RNA* **2008**, *14*, 836–843. [CrossRef]
61. Sunkar, R.; Chinnusamy, V.; Zhu, J.; Zhu, J.K. Small RNAs as big players in plant abiotic stress responses and nutrient deprivation. *Trends Plant Sci.* **2007**, *12*, 301–309. [CrossRef] [PubMed]
62. Megraw, M.; Baev, V.; Rusinov, V.; Jensen, S.T.; Kalantidis, K.; Hatzigeorgiou, A.G. MicroRNA promoter element discovery in *Arabidopsis*. *RNA* **2006**, *21*, 1612–1619. [CrossRef] [PubMed]
63. Zhao, X.; Li, L. Comparative analysis of microRNA promoters in *Arabidopsis* and rice. *Genom Proteom. Bioinform.* **2013**, *11*, 56–60. [CrossRef] [PubMed]
64. Xie, F.; Stewart, C.N., Jr.; Taki, F.A.; He, Q.; Liu, H.; Zhang, B. High-throughput deep sequencing shows that microRNAs play important roles in switchgrass responses to drought and salinity stress. *Plant Biotechnol. J.* **2014**, *12*, 354–366. [CrossRef] [PubMed]
65. Covarrubias, A.A.; Reyes, J.L. Post-transcriptional gene regulation of salinity and drought responses by plant microRNAs. *Plant Cell Environ.* **2010**, *33*, 481–489. [CrossRef]
66. Xu, Z.; Zhong, S.; Li, X.; Li, W.; Rothstein, S.J.; Zhang, S.; Bi, Y.; Xie, C. Genome-wide identification of microRNAs in response to low nitrate availability in maize leaves and roots. *PLoS ONE* **2011**, *6*, e28009. [CrossRef]
67. Fu, R.; Zhang, M.; Zhao, Y.; He, X.; Ding, C.; Wang, S.; Feng, Y.; Song, X.; Li, P.; Wang, B. Identification of salt tolerance related microRNAs and their targets in maize (*Zea mays* L.) using high-throughput sequencing and degradome analysis. *Front. Plant Sci.* **2017**, *8*, 864. [CrossRef]
68. Singh, R.K.; Shweta, S.; Muthamilarasan, M.; Rani, R.; Prasad, M. Study on aquaporins of *Setaria italica* suggests the involvement of SiPIP3;1 and SiSIP1;1 in abiotic stress response. *Funct. Integr. Genomics.* **2019**, *19*, 587–596. [CrossRef]
69. Zhu, C.; Yang, J.; Shyu, C. *Setaria* comes of age: Meeting report on the second international *Setaria* genetics conference. *Front. Plant Sci.* **2017**, *8*, 1562. [CrossRef]
70. Kozomara, A.; Birgaoanu, M.; Griffiths-Jones, S. miRBase: from microRNA sequences to function. *Nucleic Acids Res.* **2019**, *47*(D1), D155–D162. [CrossRef]
71. Dai, X.; Zhuang, Z.; Zhao, P.X. psRNATarget: a plant small RNA target analysis server (2017 release). *Nucleic Acids Res.* **2018**, *46*, W49–W54. [CrossRef]
72. Gao, P.; Bai, X.; Yang, L.; Lv, D.; Pan, X.; Li, Y.; Cai, H.; Ji, W.; Chen, Q.; Zhu, Y. Osa-MIR393: a salinity- and alkaline stress-related microRNA gene. *Mol. Biol. Rep.* **2011**, *38*, 237–242. [CrossRef]
73. Kord, H.; Fakheri, B.; Ghabooli, M.; Solouki, M.; Emamjomeh, A.; Khatabi, B.; Sepehri, M.; Salekdeh, G.H.; Ghaffari, M.R. Salinity-associated microRNAs and their potential roles in mediating salt tolerance in rice colonized by the endophytic root fungus *Piriformospora indica*. *Funct. Integr. Genomics* **2019**, *19*, 659–672. [CrossRef]

74. Bai Q, Wang X, Chen X, Shi G, Liu Z, Guo C, Xiao K. Wheat miRNA TaemiR408 acts as an essential nediator in plant tolerance to Pi deprivation and salt stress via modulating stress-associated physiological processes. *Front. Plant Sci.* **2018**, *9*, 499. [CrossRef]
75. Gupta, O.P.; Meena, N.L.; Sharma, I.; Sharma, P. Differential regulation of microRNAs in response to osmotic, salt and cold stresses in wheat. *Mol. Biol. Rep.* **2014**, *41*, 4623–4629. [CrossRef] [PubMed]
76. Han, H.; Wang, Q.; Wei, L.; Liang, Y.; Dai, J.; Xia, G.; Liu, S. Small RNA and degradome sequencing used to elucidate the basis of tolerance to salinity and alkalinity in wheat. *BMC Plant Biol.* **2018**, *18*, 195. [CrossRef] [PubMed]
77. Luan, M.; Xu, M.; Lu, Y.; Zhang, L.; Fan, Y.; Wang, L. Expression of zma-miR169 miRNAs and their target ZmNF-YA genes in response to abiotic stress in maize leaves. *Gene* **2015**, *555*, 178–185. [CrossRef]
78. Mallory, A.C.; Bartel, D.P.; Bartel, B. MicroRNA-directed regulation of Arabidopsis AUXIN RESPONSE FACTOR17 is essential for proper development and modulates expression of early auxin response genes. *Plant Cell.* **2005**, *17*, 1360–1375. [CrossRef] [PubMed]
79. Jodder, J.; Das, R.; Sarkar, D.; Bhattacharjee, P.; Kundu, P. Distinct transcriptional and processing regulations control miR167a level in tomato during stress. *RNA Biol.* **2018**, *15*, 130–143. [CrossRef]
80. Cao, C.; Long, R.; Zhang, T.; Kang, J.; Wang, Z.; Wang, P.; Sun, H.; Yu, J.; Yang, Q. Genome-wide identification of microRNAs in response to salt/alkali stress in *Medicago truncatula* through high-throughput sequencing. *Int. J. Mol. Sci.* **2018**, *19*, 4076. [CrossRef]
81. Bhardwaj, A.R.; Joshi, G.; Pandey, R.; Kukreja, B.; Goel, S.; Jagannath, A.; Kumar, A.; Katiyar-Agarwal, S.; Agarwal, M. A genome-wide perspective of miRNAome in response to high temperature, salinity and drought stresses in *Brassica juncea* (Czern) L. *PLoS ONE* **2014**, *9*, e92456. [CrossRef] [PubMed]
82. Gutierrez, L.; Bussell, J.D.; Pacurar, D.I.; Schwambach, J.; Pacurar, M.; Bellini, C. Phenotypic plasticity of adventitious rooting in *Arabidopsis* is controlled by complex regulation of AUXIN RESPONSE FACTOR transcripts and microRNA abundance. *Plant Cell* **2009**, *21*, 3119–3132. [CrossRef]
83. Liu, Y.; Li, D.; Yan, J.; Wang, K.; Luo, H.; Zhang, W. MiR319 mediated salt tolerance by ethylene. *Plant Biotechnol. J.* **2019**, *17*, 2370–2383. [CrossRef]
84. Song, J.B.; Gao, S.; Sun, D.; Li, H.; Shu, X.X.; Yang, Z.M. MiR394 and LCR are involved in *Arabidopsis* salt and drought stress responses in an abscisic acid-dependent manner. *BMC Plant Biol.* **2013**, *13*, 210. [CrossRef]
85. Sun, Z.; Wang, Y.; Mou, F.; Tian, Y.; Chen, L.; Zhang, S.; Jiang, Q.; Li, X. Genome-wide small RNA analysis of soybean reveals auxin-responsive microRNAs that are differentially expressed in response to salt Stress in root apex. *Front. Plant Sci.* **2016**, *6*, 1273. [CrossRef]
86. Yuan, S.; Zhao, J.; Li, Z.; Hu, Q.; Yuan, N.; Zhou, M.; Xia, X.; Noorai, R.; Saski, C.; Li, S.; et al. MicroRNA396-mediated alteration in plant development and salinity stress response in creeping bentgrass. *Hortic Res.* **2019**, *6*, 48. [CrossRef]
87. Zhao, B.; Ge, L.; Liang, R.; Li, W.; Ruan, K.; Lin, H.; Jin, Y. Members of miR-169 family are induced by high salinity and transiently inhibit the NF-YA transcription factor. *BMC Mol. Biol.* **2009**, *10*, 29. [CrossRef]
88. Yin, Z.; Li, Y.; Yu, J.; Liu, Y.; Li, C.; Han, X.; Shen, F. Difference in miRNA expression profiles between two cotton cultivars with distinct salt sensitivity. *Mol. Biol. Rep.* **2012**, *39*, 4961–4970. [CrossRef]
89. Jian, H.; Wang, J.; Wang, T.; Wei, L.; Li, J.; Liu, L. Identification of rapeseed microRNAs involved in early stage seed hermination under salt and drought stresses. *Front. Plant Sci.* **2016**, *7*, 658. [CrossRef]
90. Wang, M.; Wang, Q.; Zhang, B. Response of miRNAs and their targets to salt and drought stresses in cotton (*Gossypium hirsutum* L.). *Gene* **2013**, *530*, 26–32. [CrossRef]
91. Guo, X.; Niu, J.; Cao, X. Heterologous expression of *Salvia miltiorrhiza* microRNA408 enhances tolerance to salt stress in *Nicotiana benthamiana*. *Int. J. Mol. Sci.* **2018**, *19*, 3985. [CrossRef]
92. Macovei, A.; Tuteja, N. MicroRNAs targeting DEAD-box helicases are involved in salinity stress response in rice (*Oryza sativa* L.). *BMC Plant Biol.* **2012**, *12*, 183. [CrossRef]